1. Report No.	2. Government Accession No.	3. Recipient's Catalog No.
NASA CR-145140		

4. Title and Subtitle	5. Report Date
Evaluation of Mechanical Property Data on the 2219 Aluminum Alloy and Application of the Data to the Design of Liquid Hydrogen Tankage	January 1977
	6. Performing Organization Code

7. Author(s)	8. Performing Organization Report No.
W.E. Witzell	CASD-NAS-77-008
	10. Work Unit No.

9. Performing Organization Name and Address	11. Contract or Grant No.
General Dynamics Convair Division P.O. Box 80847 San Diego, California 92138	NAS 1-14048
	13. Type of Report and Period Covered Contractor Report July '75 through Dec '76

12. Sponsoring Agency Name and Address	14. Sponsoring Agency Code
National Aeronautics and Space Administration Langley Research Center Hampton, Virginia 23365	

15. Supplementary Notes

16. Abstract

The potential use of thin gauge 2219 aluminum alloy for airborne liquid hydrogen tankage was examined in this modest three-phase program. Existing data was processed using the Newman two parameter equation, a prediction was made for the life expectancy of a hypothetical liquid hydrogen tank, and additional experimental data was generated in an attempt to correct the deficiencies in the existing data.

17. Key Words (Suggested by Author(s))	18. Distribution Statement
2219-T87 aluminum alloy cyclic flow growth fracture characteristics fracture toughness fatigue 2219 alloy weldments	Unlimited

19. Security Classif. (of this report)	20. Security Classif. (of this page)	21. No. of Pages	22. Price*
Unclassified	Unclassified	88	

* For sale by the National Technical Information Service, Springfield, Virginia 22151

FOREWORD

This report describes the work performed by General Dynamics Convair Division on the suitability of the use of 2219-T87 aluminum alloy for airborne liquid hydrogen storage tanks under contract NAS1-14048 from the National Aeronautics and Space Administration Langley Research Center. The program was administered under the direction of Wolf Elber of LRC who provided technical guidance and timely advice.

At Convair the program manager W.E. Witzell was aided by C. J. Tanner and R. W. Baldi who provided all of the tank life predictions and processed the existing mechanical property data using the Newman two parameter equation.

The assistance of Dr. J.C. Newman of the Langley Research Center in providing information and tapes of his two parameter technique is gratefully acknowledged.

The experimental portion of the program was completed through the diligence of Max Spencer, Jerry Hill, Everett Wehrhan, and José Villa whose efforts and good humor are greatly appreciated.

CONTENTS

FIGURES

TABLES

1. BACKGROUND

Based upon its overall good combination of high strength/weight ratio, retention of high fracture toughness down to extremely low temperatures, excellent corrosion resistance and good weldability, the 2219 aluminum alloy has been extensively employed for liquid hydrogen tankage in one-shot launch vehicle applications. This alloy is also the leading contender for use in the liquid hydrogen tankage of long-lived transport aircraft.

An extensive amount of mechanical property data on this alloy has been developed during the past 15 years. The available data are not only essentially short time property data, but a cursory examination shows conflicting data, particularly as regards both the fatigue behavior of base metal and weld joints at cryogenic temperatures and fracture toughness properties.

It was proposed to collect, collate and evaluate the mechanical property data of thin gage 2219 aluminum alloy to determine where reliable design data exists and where additional data are needed for the design of reliable, light weight, long-lived liquid hydrogen tanks for aircraft application.

Another objective of this program was to employ the available design data on the 2219 aluminum alloy to predict the fatigue and flaw growth life of a typical liquid hydrogen tank. The tank design was based on reasonable assumptions of wall thickness and service pressure spectrum. When required data was unavailable, estimates were based upon interpolation or extrapolation of existing data.

Upon completion of the analyses and predictions, critical tests were proposed to establish the validity of the assumptions and analyses. The proposed tests were submitted for review and approval by the NASA contract monitor prior to their conduct.

During this phase of the program, gaps in the available data which were needed to support the design of reliable tankage for liquid hydrogen fueled aircraft were identified. The final phase of the program consisted of a test program to fill critical gaps in mechanical properties data on the 2219 aluminum alloy.

Objectives

1. Collect, collate and evaluate data on the mechanical properties of thin gage 2219 aluminum alloy.

2. Employ available data on fatigue and flaw growth to design and predict the behavior of a typical liquid hydrogen tank.

3. Conduct critical tests to evaluate the validity of tank design assumptions and predictions of fatigue and flaw growth characteristics, and finally, develop mechanical property required to support the design of tankage for liquid hydrogen fueled aircraft.

The principal effort was to seek data from the existing literature and to pursue new sources of information. Two data searches were initiated as follows:

(1) NASA Linear Tape Search - computer search available at General Dynamics/Convair Library and Information Services. Citations and Descriptors only.

(2) Defense Documentation Center - Search Control No. 031061 on Aluminum Alloy 2219. Citations, Descriptors and Abstracts.

The initial NASA search turned up more than 1100 references dealing with the subject area of aluminum alloys and fracture mechanics. Supplements have added an additional 700 references. The citations were examined to determine applicability to the existing program.

In addition to the two literature searches, the second supplement to the Damage Tolerant Design Handbook was obtained. The 2219 data from this document was examined and the references were checked to ensure that none have been overlooked.

2. TECHNICAL APPROACH

General

This three-phase program was designed to: (1) gather existing fracture data for very thin gauge 2219-T87 aluminum alloy; (2) use the existing data to make life predictions on a liquid hydrogen tank, and (3) supplement existing data with experimentally derived data and verify prediction methods.

Initially, collection of existing data was confusing due to the various methods of data reporting and testing. Furthermore, existing data searches proved to be incomplete and untimely. Consequently, an attempt was made to "smooth out" the available data by using the Newman two-parameter equation.

Prediction methods, while suitable for fracture analysis, were hampered somewhat by lack of clearly defined criteria for aircraft carrying or using cryogenic fluids. In thise case, a design concept was selected (without performing a complete trade-off study), and existing data was used to make the life predictions on a hypothetical thin gauge airborne liquid hydrogen tank.

Experimental programs were somewhat more straightforward, although they necessarily started toward the end of the analytical phases. A significant number of tests were planned to obtain static fracture, cyclic flaw growth and fatigue life at liquid hydrogen temperatures, as well as to provide some verification of the analytical predictions.

Analytical Studies

Three H-P 9830 computer programs have been developed to facilitate the following analysis tasks: (1) tank sizing; (2) static strength requirements and analysis; (3) stress spectrum generation, and (4) flaw growth analysis. The first of these is used to size the tank to meet volume and dimensional requirements. The second is used to establish minimum gages for static load conditions and to determine stress levels for fatigue spectra. The third is a flaw growth program incorporating Newman's Two Parameter Criterion.

Life Predictions

The H-P 9830 program was developed in about three weeks. It is less versatile than the FLAGRO program, but it does have the features necessary to conduct the present study. Run times were very slow, and it was necessary to let the machine run overnight for some spectra. A write-up and sample output of the program is given in Appendix A.

The H-P 9830 flaw growth program was used to predict flights to breakthrough for surface flaws. A number of runs were made with shortened load spectra to check out the program and establish ballpark estimates. The first run indicates that an .025-inch deep flaw in an .050-inch tank would not grow through the thickness to leak within the specified 20,000 flights. The second run predicted an .030-inch flaw would break through in 5857 flights. Run 3 included a more complex spectra with automatic generation of the ground-air-ground cycle and predicted breakthrough at 4581 flights. In Run 4 the thickness was increased to .052-inch and breakthrough occurred at 10,195 flights.

A second version of the flaw growth program was developed which includes finite width effects. This version was used to predict crack growth for the verification tests to be conducted in Phase III.

Newman's Two Parameter Approach

Through the generosity of J. C. Newman, Jr. of the NASA-Langley Research Center, this approach was adapted to the present program. The original program was modified slightly and a tape was generated for the H. P. 9830. This program was used to process static fracture data.

At the same time, a program, FLAGRO, originally generated by Rockwell International for use on the Space Shuttle, was examined for applicability of the two parameter approach. However, after several days of effort, it became obvious that this approach would require a considerable effort and was beyond the scope of this program. We have made minor modifications to the programs to speed up the input and improve the print out. Also, we have changed the K_f and m program to allow net section stresses up to the ultimate strength of the material. All values of K_f and m calculated from tests in which the net section stress exceeded yield strength were flagged. This change was necessary to obtain K_f and m values for 2219-T87 welds. All data we have reviewed for this material showed the net section stress at failure to be higher than yield. This also occurs quite frequently in parent material tests at the higher temperatures.

Phase II

Tank Sizing

To varying degrees, sizing of the liquid hydrogen tank is dependent on material property data availability, identification of the operating conditions of the vehicle, existing government requirements for airplane construction, and the availability of suitable load and pressure spectra.

This program attempted to come to grips with the requirement of material property data, but precise solutions for the other conditions were beyond the scope of this program. Nevertheless, each of these was addressed in the sizing of the tank itself. For example, a load/pressure spectrum was generated that was general in nature to account for typical conditions that a commercial airplane may experience. Definition of this modified spectrum was difficult due to various factors, one of which was the design selection of integral or non-integral tanks.

Initially, a general cylindrical tank was sized (manually) under static load conditions assuming a non-integral tank. The structural requirements as set forth in FAR4B Part 25 (Commercial Airplane Design) were used recognizing that at the time that document was prepared, the possibility of liquid hydrogen containment was not considered. It was assumed that the tank would have to be guaranteed for twice the expected operating pressure in the same manner as--say cabin pressure, although current cryogenic tank design does not make that assumption.

The manual approach has been programmed for a more general case that has been adapted to the H. P. 9830 computer.

The present study was not primarily concerned with evaluation of aircraft configurations. The objective was to evaluate the availability of data and methods needed to design the LH_2 fuel tanks. Trial analyses of the two types shown in Figures 1 and 2 should be adequate for this tudy program. Type I was selected because it appears to be a minimum weight configuration, and is relatively insensitive to flight inertia loads. Thus only ground-air-ground cycles are important in fatigue and crack growth analyses. Type II was selected because it is very sensitive to flight loads and the analyses will emphasize their effects on fatigue and crack growth.

Table 1 was a preliminary output of the H-P 9830 program used to size the tanks. Volumes and dimensions are consistent with configurations defined in a previous study (NAS1-12972) for a 400 passenger, 5500 n. mile transport.

The program sizes cylindrical tanks with hemispherical, ellipsoidal, or conical end bulkheads (see Figure 3). Volumes, surface areas, weights, and centroids are output. This data was needed as input to the LH_2 Tank Stress program described below.

Static Strength Requirements and Analysis

In trying to establish tank gages and stress levels for static load conditions, a major problem arose. The structural criteria used to design conventional transport aircraft are not appropriate for LH_2 fueled aircraft. Realistic and adequate factors for proof pressure, operating pressure, burst pressure, limit loads, ultimate loads, emergency landing loads, and combinations can be set only after their impact on weight, reliability, safety, service life, and costs has been determined. A thorough study of these relationships was not within the scope of the present work. The following preliminary criteria were assumed for this study.

Loads and Criteria

Structural requirements for transport airplanes are given in Federal Aviation Regulations Part 25. The following will serve in establishing LH_2 tank gages. (Specific requirements for LH_2 tanks would have to be formulated before an LH_2 airplane could be certified.)

Maneuver Inertia Factors: (Ref. FAR p. 25.333)

N_z = 2.5 Limit @ c.g.
N_z = -1.0 Limit @ c.g.

Gust Loads: (Ref. FAR p. 25.341)

(See para. 3)

Emergency Landing Inertia Factors: (Ref. FAR p. 25.561)

Upward:	2.0 g
Forward:	9.0 g
Sideward:	1.5 g
Downward:	4.5 g

Cabin Pressure: (Ref. FAR p. 25.365, p. 25.841, p. 25.843)

P_{op} = 2438 m altitude + relief valve + aero. force $\simeq$ 62.76 KN/m^2 (9.1 psig)

$P_{lim} = P_{proof} = 1.33\ P_{op} = 83.47$ KN/m^2 (12.1 psig)

$P_{ult} = 1.5\ P_{op} = 94.14$ KN/m^2 (13.65 psig)

$P_{burst} = 1.5\ P_{lim} = 2.0\ P_{op} = 125.52$ KN/m^2 (18.2 psig)

Fatigue, Failsafe, and Residual Strength: (Ref. FAR p. 25.571)

(See para. 3)

Engine Explosion, Lightning, Bird Strike, etc.

TBD

LH_2 Tank Design Pressures

Vented LH_2 tanks have been designed to operate at pressures in the range of 138 KN/m^2 (20 psia) to 207 KN/m^2 (30 psia). In this study an intermediate value 172.5 KN/m^2 (25 psia) is used. Factors required for cabin pressure are assumed applicable to LH_2 tank design and the maximum cruise attitude is assumed to be 13716 m (45000 ft).

P	$= 172.5$ KN/m^2	(25 psia)	
P_{at}	$= 101.4$ KN/m^2	(14.7 psia)	@ S.L.
P_{at}	$= 14.8$ KN/m^2	(2.14 psia)	@ 13716 m (45000 ft.)
ΔP_{sl}	$= 71.1$ KN/m^2	(10.30 psig)	
ΔP_{alt}	$= 157.7$ KN/m^2	(22.86 psig)	
P_{op}	$= 1.1 \times 157.7 = 173.47$ KN/m^2	(25.14 psig)	
P_{lim}	$= 1.33 \times P_{op} = 230.72$ KN/m^2	(33.44 psig)	
P_{proof}	$= 1.33 \times P_{op} = 230.72$ KN/m^2	(33.44 psig)	
P_{ult}	$= 1.5 \times P_{op} = 260.21$ KN/m^2	(37.71 psig)	
P_{burst}	$= 2.0 \times P_{op} = 346.94$ KN/m^2	(50.28 psig)	

NOTES:

1. For proof tests conducted at room temperature the proof factor is $1.33\ (F_{ty_{RT}} / F_{ty_{OP}}) = 1.33\ (51/66) = 1.03$
2. For Type I tank compartment is assumed pressurized to 34.5 KN/m^2 (5 psig).
3. A factor of 1.1 on operating pressure is assumed to account for relief valve tolerance and aerodynamic suction.

LH_2 Fuel Tank Stresses Program

A preliminary design type of computer program was written to determine gages and stresses for static load conditions. Only tensile stresses due to ullage gas pressure, head pressure, bending moments, and axial loads are treated. Additional failure modes would have to be considered in a real design effort. Input to the program consists of the preceding criteria, output from the tank sizing program, and tensile strength properties. The program calculates required thickness at six points (Fig. 3) for ten conditions. The maximums are saved and printed out as required thickness. A second pass is then made through the ten conditions and stresses are printed out. Some of the conditions were chosen to facilitate the development of fatigue stress spectra. A preliminary output for tank Type I is shown in Table 2.

3. Stress Spectrum Generation

Table 3 is a preliminary stress spectrum for tank Type I, analysis point 3H. (See Figure 3) Occurrences of taxi, gusts, and maneuver cycles were obtained by factoring values given in NASA-CR-132648, Table 2-2. Occurrences in cruise segments were ratioed up to reflect a 5 hours flight instead of a 1.43 hour flight. Other occurrences are more dependent on climb and descent and therefore not changed by the flight duration. Stress magnitudes were found by adding or subtracting appropriate Δg values to the output of the LH_2 Fuel Tank Stresses program. (See Table 2.)

Also, the following assumptions are made regarding life requirements:

1. Tank life = 50,000 hrs.
2. Flight duration = 5 hrs.
3. Flights per life = 10,000
4. Flights per block = 1,000
5. Proof test per block = 1
6. Leak test per block = 10
7. Scatter factor on life = 2

Phase III

Experimental Program

General

The experimental portion of the program consisted of two parts, namely: (1) a prediction verification portion, and (2) data generation to supplement existing data. Phase III started in the latter stage of Phases I and II, but due to schedule constraints, had to be planned well in advance of the completion of those phases. Consequently, some degree of uncertainty was built into the experimental phase. For example, in the early stages of Phase I, it was not known whether additional conventional fatigue data was needed. In this case, a small quantity of fatigue tests were scheduled for testing at -423°F.

Furthermore, it was known that other programs were being conducted to generate additional data (e. g. , NASA sponsored programs at Martin and Boeing), but neither of these had progressed to the stage where published data was available, nor was it certain that the data would be applicable to the existing program.

The experimental program that evolved made an attempt to examine the overall efficiency of the predictive method in a non-statistical sense and to supplement existing data in certain critical areas where it appeared that sufficient data was not available at the time that the predictions were made.

Verification Testing

The verification test portion made use of surface notched fracture specimens that were . 127 cm (0. 040 in.) (nominal) thick in a chemically milled condition and were . 318 cm (0. 125 in.) thick in the welded condition. In order to eliminate another variable, the chem milled specimens were fabricated from the same 0. 125 in. base material from which the weldments were made. Chem milling was performed by the Chem Energy Company of San Diego using a standard production bath for aluminum alloys without masking.

Three specimens were tested at room temperature at the beginning of the program in order to check out the experimental technique as well as to gain some knowledge as to whether the predictive and experimental methods were reasonably compatible. The tests were designed to examine the effect of three inspection interval design concepts, which were: (1) no proof testing during the expected life of the tank, (2) a single proof test prior to the first flight, and (3) a proof test every 1000 flights.

Since design of the proof test criteria was beyond the scope of this program, and since no effective proof test scheme to screen out critical flaws in very thin walled tanks is known to the author, the selection of the proof test stress was somewhat arbitrary. In lack of a more rigorous fracture mechanics proof test scheme, the structural design criteria of 1.03 times the operating stress (room temperature) was used for the proof test stress.

To a large degree, the load spectrum on the specimen was a function of the design philosophy of liquid hydrogen tankage in a transport type aircraft. Again, the actual design concept is beyond the scope of this program, but the selection of a non-integral tank over the integral tank has merit in both the operating aircraft philosophy and in the simplicity of the verification testing.

Use of the "floating tank" concept reduces the significant load consideration to that of tank pressurization while minimizing other loads due to such forces as flutter, gusts, etc.

As has been explained, the spectrum can be simplified to a single excursion of stress from 145 MPa (21.0 KSI) to 310 MPa (45.0 KSI) for the base metal, and from 57.9 MPa (8.4 KSI) to 124 MPa (18.0 KSI) for the weldments. In the actual flight conditions, the load applications would be of rather long duration, but for purposes of testing, it is much cheaper to apply the loads at a faster rate. It has been the experience of recent investigators (including Convair) that if there is a frequency effect that is influenced by an aggressive environment, the effect is noticed at frequencies less than 10 Hz. Consequently, two frequencies were examined, namely: 1.0 Hz and 0.1 Hz. Since there is very little evidence that liquid hydrogen attacks 2219 aluminum alloy in a hostile environment framework, no difference was expected between the two frequencies and the tests at the lower frequency were minimized. It should be mentioned, however, that sustained load crack growth in liquid hydrogen should not be ruled out, although such a condition may be minimized by keeping the applied crack intensity factor below the sustained load threshold of 2219 aluminum alloy in liquid hydrogen. (Insufficient data was available in this area. If long term storage of liquid hydrogen is to be considered, this data should be generated in another program before the design concept is locked in.)

Data Generation

In the early stages of the data collection and evaluation phase, it was determined that there was little data available on 2219 aluminum alloy in very thin gauges. Even so, it was felt that the small amount of data would be usable

and consistent when it was modified by the Newman two parameter scheme. However, some of the data--particularly for weldments--was so inconsistent that the information was not usable no matter how it was modified.

The data generation phase of the program was designed to fill the voids as much as possible. However, because of the somewhat limited scope of this phase, the results obtained are not of statistical significance. If this data is added to existing information and to other data being generated at this time, it should be of value to designers.

As has been discussed, there was very little data available on thin gauge 2219 aluminum that had been chem milled. Consequently it was desirable to obtain static fracture and cyclic flaw growth for this material at both room temperature and 20°K (-423°F). At the same time, it was necessary to obtain similar information on the weldments. However, it is likely that the weld land region in a liquid hydrogen pressure vessel would be significantly thicker than the parent material. Therefore, the welded specimen was not chem milled, and was in the as-received condition and thickness. The as-received material was designated as 2219-T87 aluminum alloy.

A minimum number of tensile tests were performed in order to establish the strength level of the material under test, and to determine if the chem milling had a noticeable affect on the mechanical properties of the parent material. During the data collection and evaluation phase, it was noted that standard fatigue data was not available for this alloy at liquid hydrogen temperature. Inasmuch as Convair has one of the few facilities in the country for generating such data, it was decided that a minimum number of tests should be performed to ascertain if any peculiar fatigue properties were present for either the chem milled or welded material (See Figure 4).

A total of 86 tests were scheduled for the data generation phase of which 56 were to be tested in liquid hydrogen.

Tensile Tests

Mechanical properties tests were performed on conventional flat tensile specimens in order to determine the strength of the chem milled material and weldments. Properties were obtained for both longitudinal and transverse grain directions of the 0.050 in. (nominal) thick material at room temperature and 20°K. Originally the weldments were to be tested in the as-received 0.125 in. (nominal) thickness only. However, some weldments of the thinner chem milled material were obtained and two specimens were tested at 20°K.

Tests were performed in a Tinius Olsen 30,000 lb. Universal test machine using a Class B-2 extensometer. Tests at 20°K were enclosed in a General Dynamics developed cryostat (Figure 5) installed in the test machine. Stress-strain curves were obtained autographically in order to obtain tensile yield strength and modulus of elasticity. Elongation was obtained over a two-inch gage length.

Material

The material to be considered for this program was 2219 aluminum alloy in the cold stretched and aged condition, designated T-87. This aerospace material was designed for cryogenic usage and has been proposed and used for many of the major assemblies of the Space Shuttle. Prior to the Shuttle usage, it was used for several one-shot vehicles that utilized liquid hydrogen as a fuel and liquid oxygen as an oxidizer.

Characteristics of the material that make it attractive include good strength-to-weight ratio, good weldability, and adequate cryogenic properties. A limited amount of data indicate that the material has good toughness and resistance to stress corrosion crack. As with most materials, the toughness varies with thickness and temper. Furthermore, welding reduces the yield strength significantly and has an effect on the fracture toughness. The effect of chemical milling on toughness is generally unknown.

Welding

In general, the 2219-T87 aluminum alloy was welded in the full as-received thickness of 0.125 in., although several weldments of the chem milled material were also made. The gas tungsten arc (GTA) method was used with 1/16 in. 2319 aluminum alloy filler wire. The material was cleaned per MOS-1-02801-003, hand scraped and draw filed per 76Z1919.

Specimens were machined from several sheets of the 2219-T87 aluminum alloy. One sheet was laid out as shown in Figure 6. The other sheet was sheared into 2 ft. x 4 ft. panels in order to facilitate chem milling.

Prediction Verification

Prediction verification tests were performed on part through crack specimens with a specimen width of 4 inches (10.16 cm) a surface crack length of approximately 0.20 inch (5.08 cm), and an aspect ratio of 0.1. Flaws were induced with an electrical discharge machine (EDM) and extended by a low stress combination of tension-tension and flexural fatigue.

As mentioned, three types of proof loads were applied to the specimen. In the first case, no proof load was used at any time during testing. In the second case, a proof load of 1.03 times the operating maximum load was applied prior to the flight spectrum cycling. The third sequence required interrupting the flight spectrum after each 1000 flights and applying a single rppf load of 1.03 times the maximum flight load.

Half of the specimens were cycled at a frequency of 1.0 Hz and the remainder were cycled at 0.1 Hz. During cycling periodic visual observations were made of the back surface of the specimen in order to determine the time (cycles) that the surface flaw penetrated the back surface. After break through (if it occurred) cycling was continued until fracture occurred. In the case of the welded specimens, if no crack growth was detected in approximately 100,000 flights, cycling was discontinued.

Plane Stress Crack Intensity Factor

In order to obtain static fracture toughness data at room temperature and 20°K, center through cracked specimens (Figure 7) were tested in both parent metal and welded conditions. Specimens were pre-cracked in tension-tension fatigue at room temperature at gross stress levels below 20 percent of yield strength of the material.

Tests were performed in a Tinius-Olsen tensile testing machine. For tests at 20°K, a cryostat equipped with a viewing port was used. All base metal test specimens were machined from 2219-T87 sheet that was chem milled from a thickness of 0.318 cm to a nominal thickness of 0.127 cm.

Weldments were made using conventional gas tungsten arc (GTA) techniques on the as-received 0.318 cm material. (Note: Several additional welded specimens were tested that were obtained from a Convair IRAD study on chem milled 2219-T87 in the 0.127 cm thickness range.)

Cyclic Flaw Growth Tests

Flaw growth (dl/dN) was obtained utilizing center notched specimens (Figure 7). As for the static fracture toughness tests, data was obtained for both the longitudinal and transverse grain directions of the chem milled parent material and for the welded (GTA) material in the as-received 0.318 cm thickness. Specimens were pre-cracked in tension-tension fatigue at a frequency of 30 Hz at room temperature. The general procedure for room temperature and liquid hydrogen testing was the same, although somewhat more data points were obtained at room temperature than at 4°K.

Loads were applied in ascending order so as to minimize the possibility of crack retardation. For a given load several crack length readings were obtained before proceeding to the next larger load. No attempt was made to "mark" the crack front by frequency or amplitude changes since the direct visual observation technique is quite satisfactory for very thin gauge materials. While allowing the crack to grow increases the applied crack intensity factor, the difference is quite small and an increase in load is necessary to provide a spread in the data.

The tests were performed on a Tatnall Servo Controlled hydraulic test system at a frequency of 1 Hz. When liquid hydrogen tests were performed, a Convair developed cryostat with a viewing port was installed in the test system (Figure 8).

3. RESULTS

General

Results are presented for the three phases of the program in several ways. Phases I and II were involved with analytical studies and are mixed together to a certain degree, while the Phase III (Experimental) results are shown in the form of raw data reduced to typical tabular or curve form. The initial phases utilized existing data prior to the start of the experimental phase, but no attempt was made to fit the new data into the original analysis or prediction programs. It would be prudent to use the experimentally derived data to modify the existing predictions, but this was beyond the scope of the program.

Some by-products of this project were several HP 9830 computer programs and a bibliography on 2219 aluminum alloy that appear in the appendix of this report. The experimental program was significantly broadened (with the NASA approval) over the original work statement principally because of the lack of availability of satisfactory thin material data.

Analytical Studies

Newman fracture criterion parameters K_f and m obtained from reduction of data obtained from the literature search are presented in Tables 4 through 9. As shown, both surface- and through-cracked specimens of various widths, flaw sizes, thicknesses, temperatures, and crack propagation directions have been included.

A relationship between K_f and m versus thickness was found to exist for some groups of data. However, this relationship generally existed only for the data for which net stress at fracture was less than yield stress. Plots of both K_f and m versus thickness for most of the available data are presented in Figures 9 through 16. Curve fitting was conducted on those data plots for which a relation with thickness clearly existed. Least squares curve fitting was employed based on a modified version of the HP 9830 Math Pac polynominal regression routine. Only those data points which satisfied the criterion on (net stress / yield stress) were included. For those data groups in which the net stress at fracture was generally greater than yield stress, no relationship was found.

Average values of Paris type growth equation coefficient (C and n values) were computed from the available da/dN data for stress ratio (R) equal zero. A best fit straight-line approximation of the da/dN data was used for coefficient determination.

Estimates of ΔK_o (cyclic threshold intensity) values were derived from available data. It was found that ΔK_o increases with a decrease in temperature for the parent material.

A preliminary summary of the parameters to be used for fracture analysis predictions is shown in Table 10. The parameters presented include estimated values based on extrapolations of available data.

Some of the more important data sources are shown in Table 10a.

Prediction Verification

Two tests were performed at room temperature to check out the experimental technique and for an early check of the prediction method. The first test utilized a stress ratio (R) of +0.1 and was continued until fracture occurred. The second test used the spectrum of 144.8 to 310.3 MPa as required by the program and the cycle at which break through and subsequent fracture occurred was recorded. Since the technique seemed satisfactory, it was adopted for the liquid hydrogen tests (Table 11). Except for specimen L5, crack through occurred at between 2400 and 3675 flights (cycles), which is reasonably consistent considering the inaccuracies in obtaining accurate crack depths during pre-cracking.

In the case of welded specimens, using a spectrum excursion of 57.9 to 124.1 MPa no break throughs were obtained in less than 100,000 flights.

Summary of Properties Tests

During the search for adequate data under Phase I, it became obvious that insufficient data was available for thin gages at 20°K. In the case of the potentially important sustained load crack growth at 20°K, there was no data. Consequently, additional properties were generated for strength, toughness, cyclic crack growth, and fatigue. A comparison of tensile properties shows the expected trends:

	Tensile Yield (MPa)	Tensile Ultimate (MPa)	Weld Yield (MPa)	Weld Ult. (MPa)	Chem Mill Weld Ult. (MPa)
R.T.	385	460	135	262	-
20°K	506	684	249	458	471

The increased strength with cryogenic temperature is expected. The relatively low weld yield/ultimate ratio is also expected. The somewhat stronger weld strength for the chem milled material was not expected.

Similar trends are noted for fracture toughness (MPa $\sqrt{m}$).

	K_c (long.)	K_c (trans.)	K_c (welds)	K_c (chem mill welds)
R.T.	50	47	33	33
20°K	69	68	45	47

Again, the properties increase with a decrease in temperature, and the weldment is less tough than the base metal. However, chem milling has very little effect on toughness of the weld.

Comparisons for cyclic crack growth are more difficult. However, if all the ΔK vs da/dN curves are compared, virtually all points fall within the same scatter band. Conventional fatigue data in a liquid hydrogen temperature is also very difficult to find. However, the results obtained show greater life for corresponding stresses at 20°K than do room temperature results for thicker materials. As with other tests, the welded material shows inferior properties to the base metal as shown below.

Stress (MPa)	B.M. (Cycles)	Weld (Cycles)
450	2.6×10^5 (est.)	2×10^3
400	5×10^5 (est.)	2.5×10^4 (est.)

Tensile Tests

Mechanical properties were obtained for both the chem milled base metal and for the TIG weldments at room temperature and 20°K (Table 12). Weld strengths were obtained primarily in the as-received thickness of 0.125 inch (. 318 cm), although several tests were also performed on the chem milled material.

As expected tensile yield and ultimate strength for both the base metal and weldments were higher at 29°K than at room temperature. Also, the strength values for the weldments are significantly lower than for the base metal. An indication of the cryogenic toughness of the base metal is shown by the elongation of the material which shows no degradation at 20°K. On the other hand, the elongation of the weldments are somewhat lower.

There appears to be some effect of chem milling on the weld strength, although with such a small sample size, it may be simply a statistical anomaly.

Static Fracture Toughness

Static plane stress critical crack intensity factors were obtained for the base material and weldments at room temperature and 20°K (Tables 13 through 17) using center notched fracture specimens. Values were obtained for both longitudinal and transverse grain directions for the base material in the chem milled condition. The bulk of the weldments were in the as-received thickness of 0.318 cm in the longitudinal grain direction. Plane stress critical crack intensity factor was obtained using the following equation:

$$K_c = \sigma \sqrt{\pi a \sec \frac{\pi a}{W}}$$

where a = half crack length

W = specimen width

σ = gross stress

The gross stress and K_c for the longitudinal grain direction was slightly higher than for the transverse grain direction. As expected, the plane stress fracture toughness was less for the weldments than for base metal.

Cyclic Flaw Growth

Of all the data required for this material with respect to its use as an airborne liquid hydrogen storage tank, the cyclic flaw growth data was the most difficult to find in the proper thickness, and was the most expensive to obtain experimentally. Part of the problem for obtaining this information at liquid hydrogen temperature is concerned with obtaining the crack growth while the specimen is immersed in the cryogenic fluid due to the lack of an automatic crack measuring instrument.

Various techniques have been devised to measure such changes as crack-opening-displacement (COD) and relate that to crack length. In most cases, however, the COD has to be calibrated against crack length in the environment in which the test is to be run. In this case, the environment was liquid hydrogen which would have required an extremely expensive and time-consuming calibration. Furthermore, the continual operation of a strain gaged compliance gage under fatigue loading in a liquid hydrogen environment is a marginal condition at best.

Consequently, crack growth rates for the thin gauge 2219-T87 aluminum alloy were laboriously obtained by periodic visual observations through a viewing port using a suitable scale superimposed on the fracture specimen. Periodically, the load was increased in order to spread the final data while maintaining the stress ratio (minimum stress/maximum stress) of +0.1 for the nominal gross stress on the specimen. Data was reduced using the equation

$$\Delta K = \frac{\Delta P}{BW} \sqrt{\pi a \cdot \sec \frac{\pi a}{W}}$$

where $\Delta P = P_{max} - P_{min}$

and P_{max} = maximum applied load

P_{min} = minimum applied load

The range in applied stress intensity factor (ΔK) was calculated using the crack length at the beginning and at the end of a measured crack interval. These two values were averaged for plotting in the crack growth rate curves (Figures 17 through 24). It is recognized that such an average does not give a precise value, but if the crack growth interval is small, the resultant error may be neglected.

The crack growth rate curves were constructed in the same general manner as those presented in the Damage Tolerant Design Handbook (MCIC-HB-01) on a log-log scale. Where practicable, the results from several tests are plotted on the same curve.

In general, the scattering of data seems to compare favorably with other data presented in MCIC-HB-01. Occasionally, a data point seems to be out of sequence, i.e., the crack growth rate for a larger ΔK seems to be less than for the smaller ΔK. This is probably due to inaccurate reading of a single crack length or the propensity of a crack to grow erratically in "fits and starts."

Fatigue Tests

Conventional fatigue tests were performed on parent material and weldments. Both longitudinal and transverse grain directions were examined in the parent metal condition while only the longitudinal direction was tested in the welded condition. All tests were performed in liquid hydrogen (20°K) at a stress ratio (R) of 0.1 at a constant frequency of 30 Hz.

Results of all tests are shown in the S-N diagram (Figure 25). No attempt was made to obtain an endurance limit because of the expense of this type of testing in liquid hydrogen and because of the lack of application for the expected service.

As expected, the stress required to cause failures for weldments was considerably lower than was that of the parent material. Furthermore, the weld tests provided a large amount of scatter. Unfortunately, scatter is an expected evil in fatigue testing. In addition, testing in liquid hydrogen causes additional spreading of test data probably due to accentuating of defects in the material. Add to these factors the relative inconsistencies of weldments, and the results obtained seem quite reasonable.

4. CONCLUSIONS

1. Although the cryogenic alloy 2219-T87 has been in use for a number of years, there is still insufficient data for complete evaluation of cryogenic structures under certain conditions. The very thin material and the welded alloy in sheet conditions at 20°K have not been evaluated sufficiently to provide good statistical data. Of particular concern is the sustained load crack growth rates of 2219-T87 at 20°K.

2. For a "floating" tank containing cryogenic fluids on board a transport airplane, it is possible to predict the service life using fracture theory, providing that the weldments are conservatively designed and that the ultimate failure load is defined. However, the pressurization history of the tank between flights must be such that the resulting stress is below the sustained crack growth threshold at the temperature of the cryogenic fluid.

3. Additional data was generated to supplement the sparse information that was identified in paragraph one. These include plane stress fracture toughness, cyclic flaw growth, and fatigue properties of 2219 aluminum alloy in chem milled and welded conditions at room temperature and 20°K.

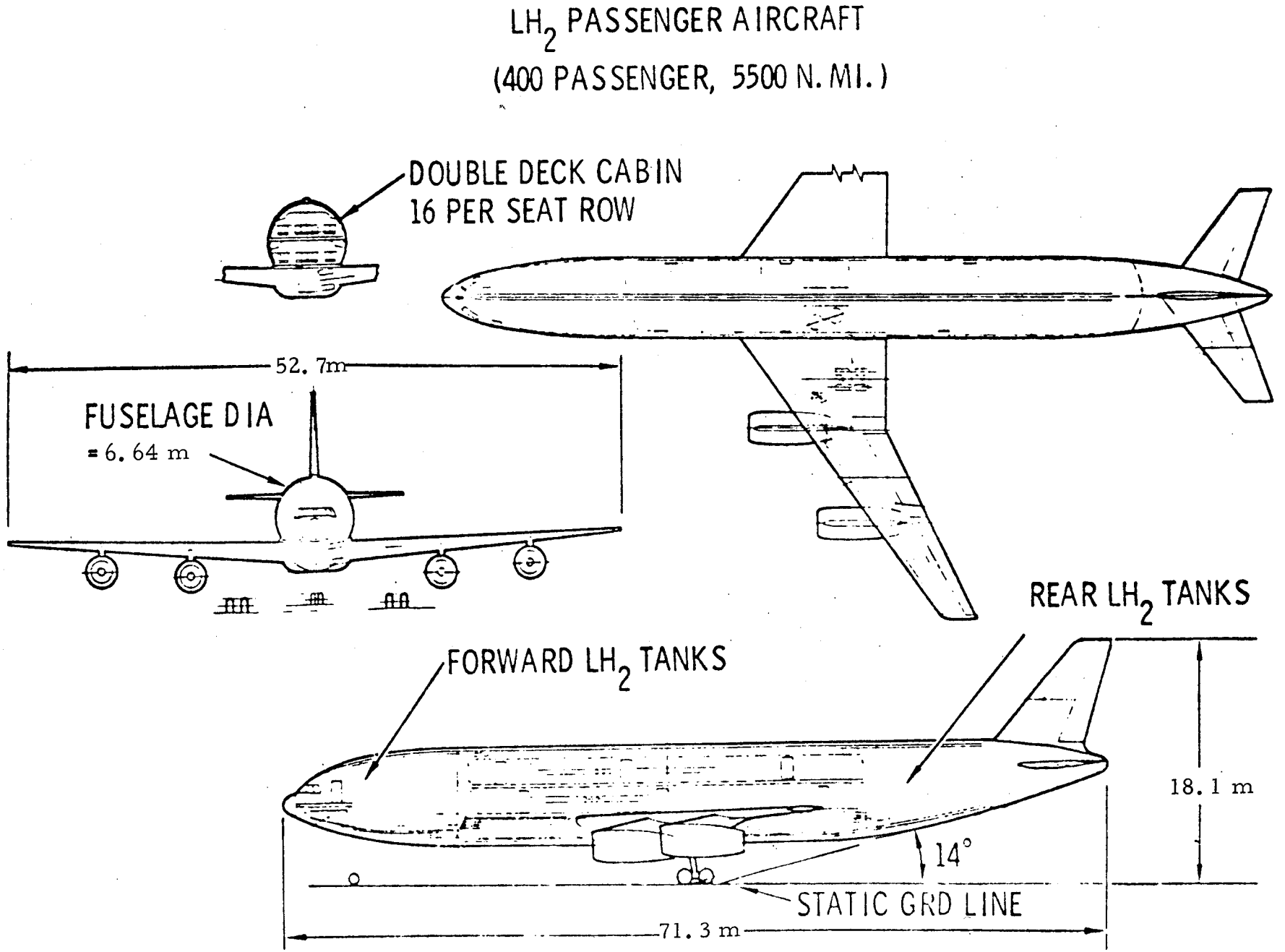

Figure 1. Selected Internal Tank Configuration — Type I

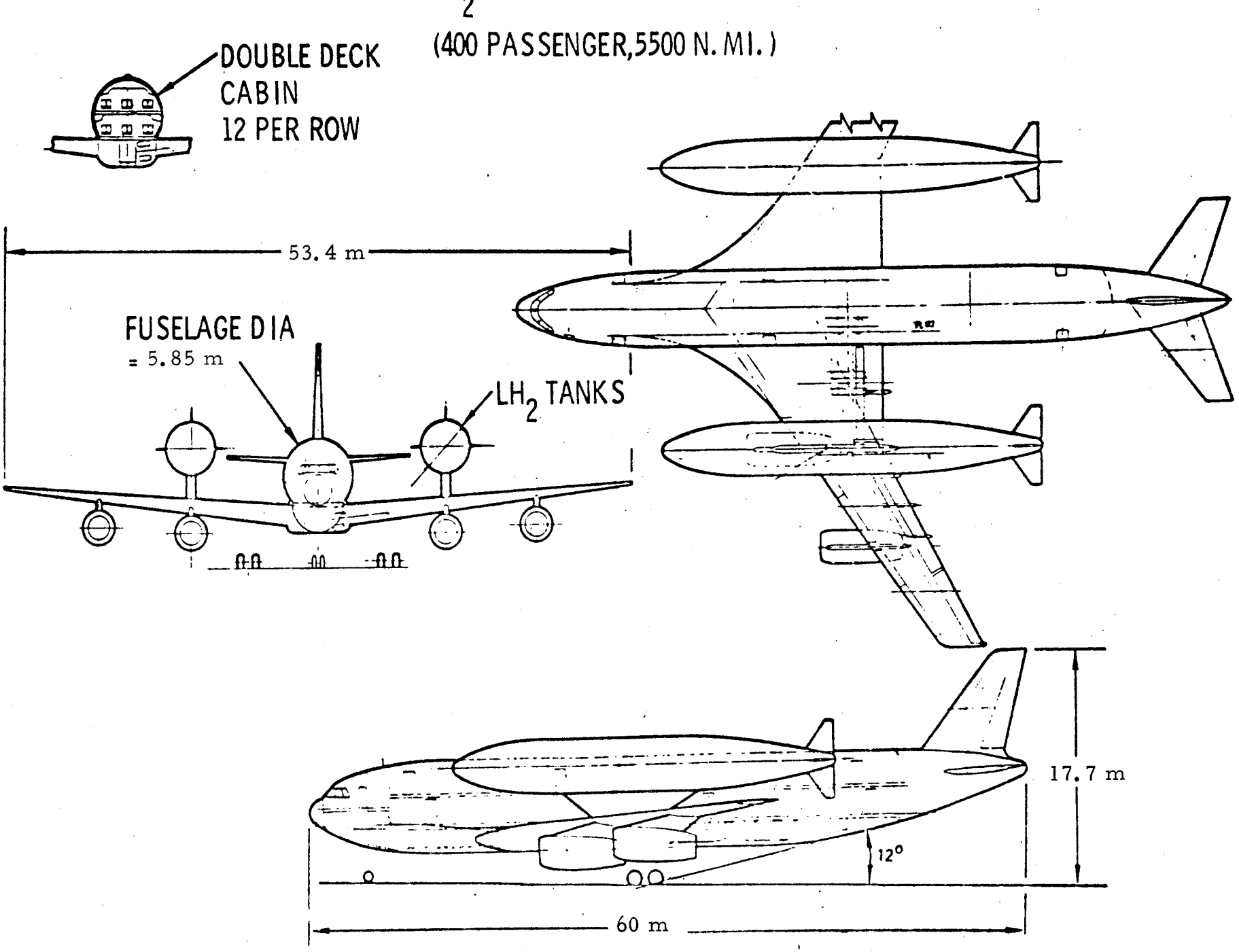

Figure 2. Selected External Tank Configuration — Type II

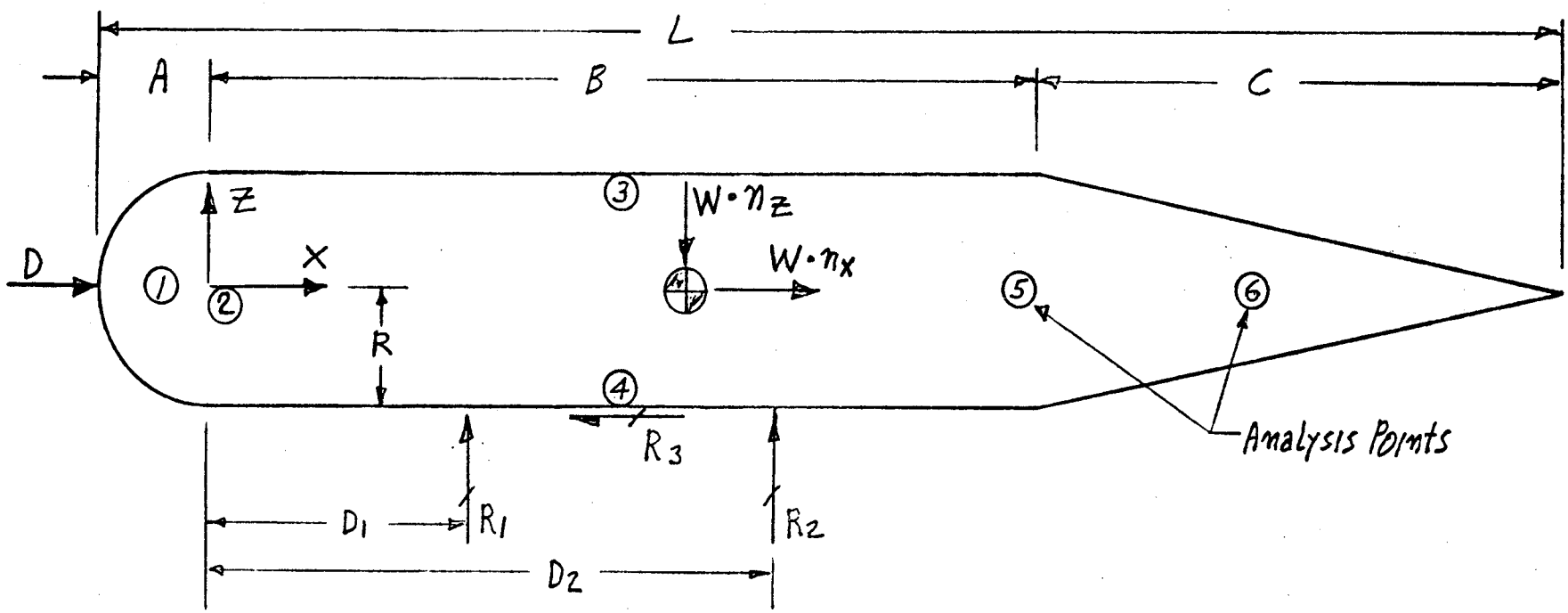

Note: End bulkheads may be hemispherical, ellipsoidal, or conical

Figure 3. LH_2 Fuel Tank Geometry

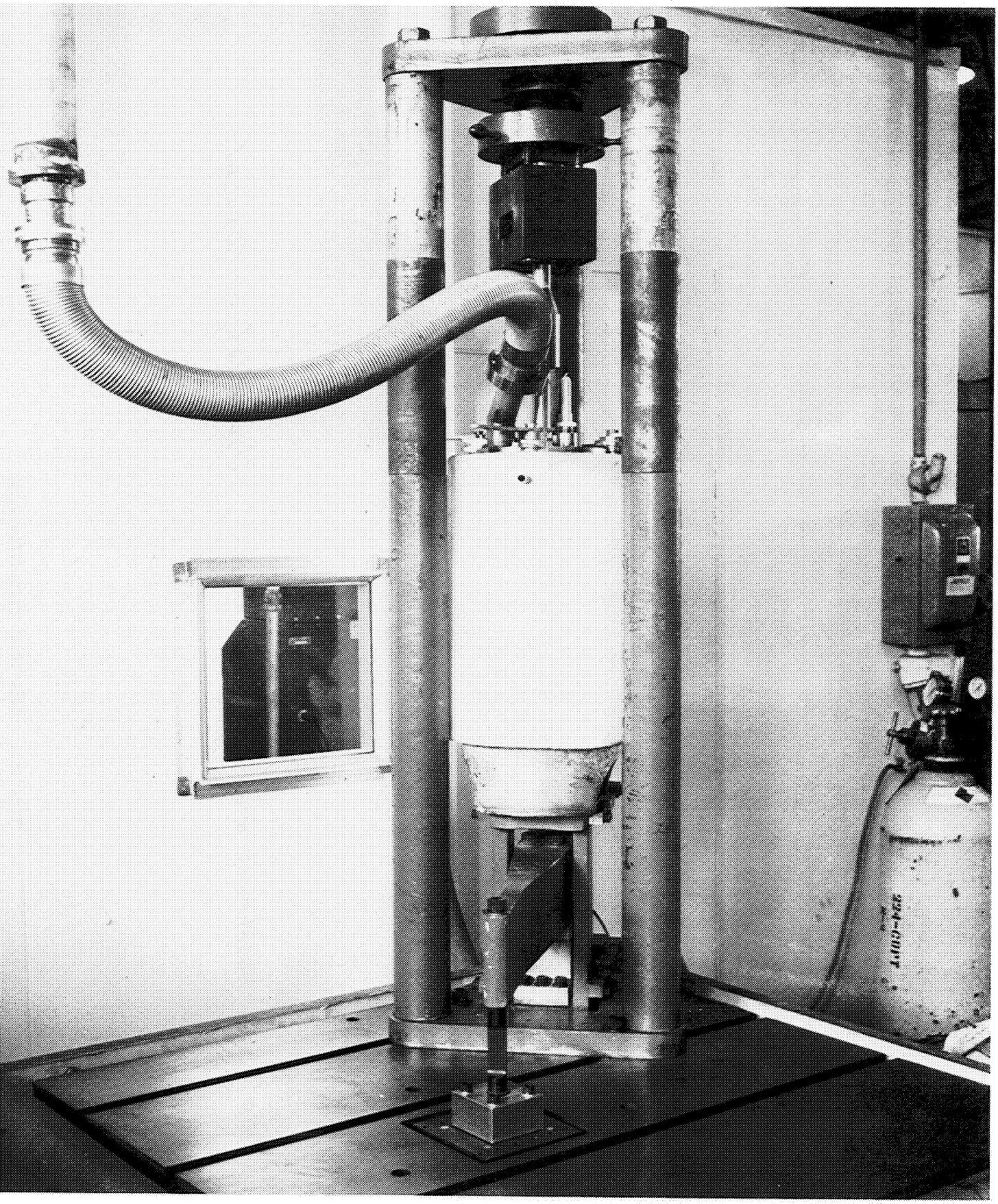

Figure 4. General Dynamics/Convair Developed Liquid Hydrogen Cryostat in Modified Constant Amplitude Fatigue Machine (Photo No. 15 4142)

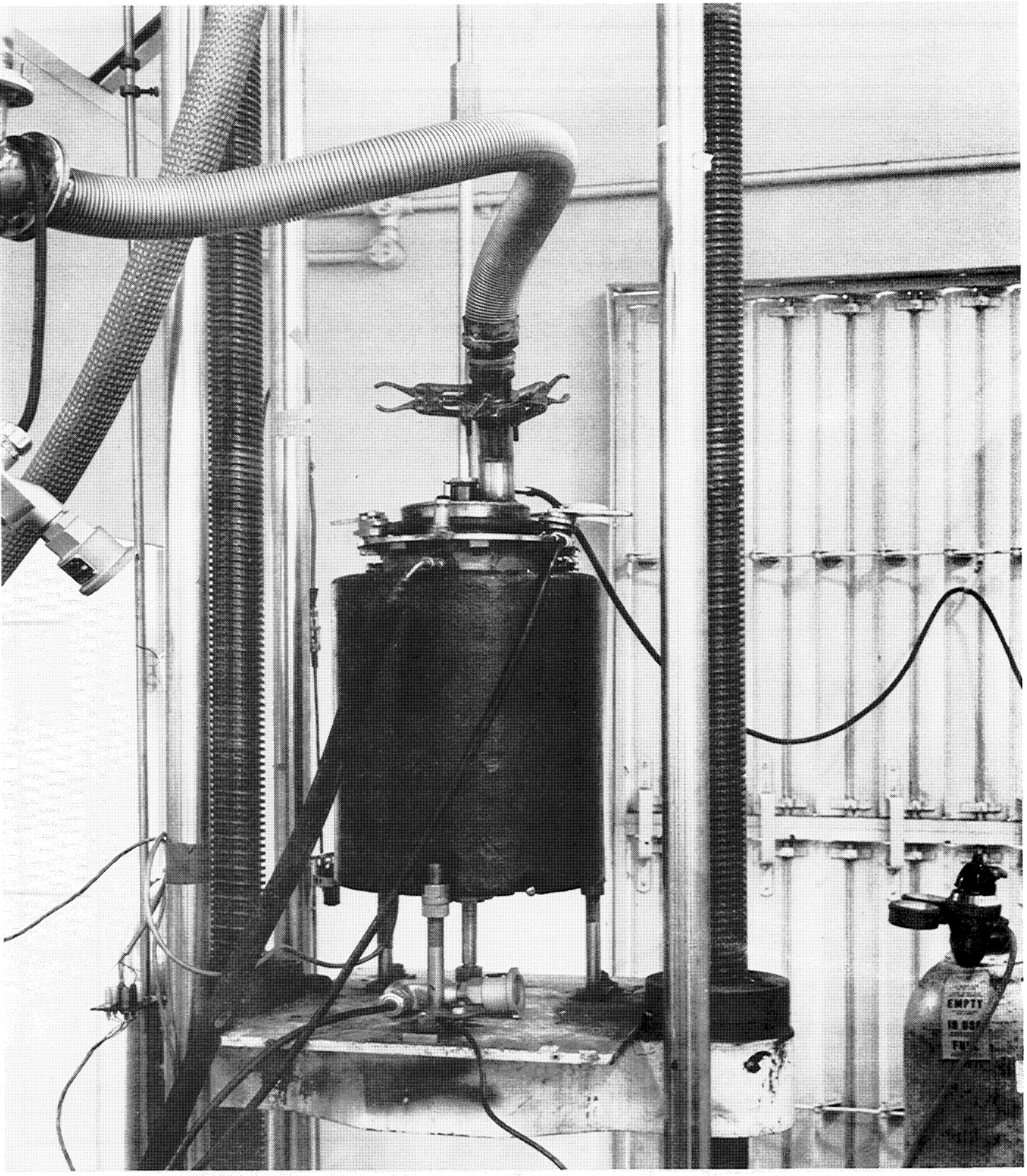

Figure 5. Liquid Hydrogen Cryostat Installed in Tinius Olsen Tensile Test Machine

(Photo No. 139373)

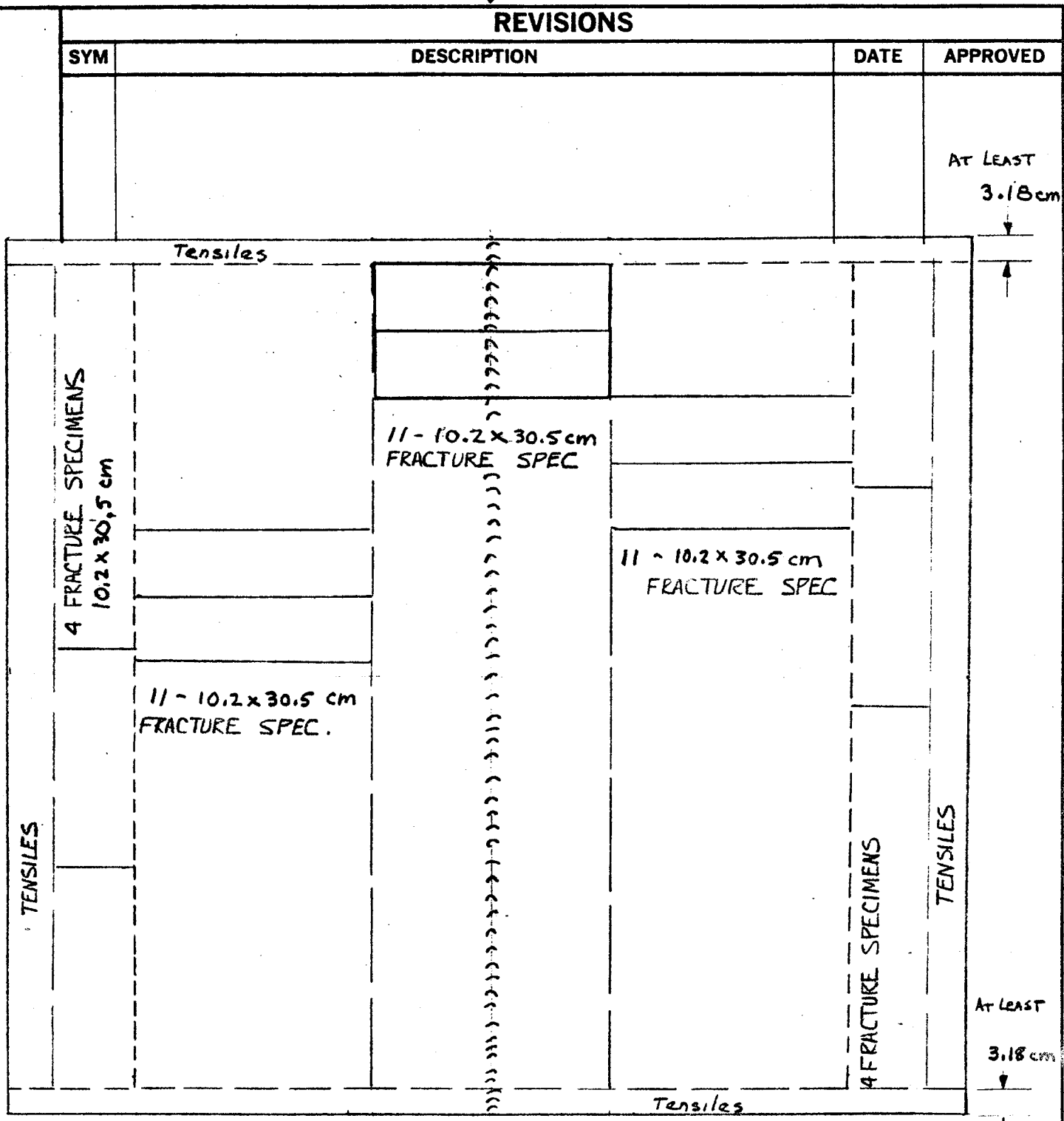

Figure 6. Layout of Tensile and Fracture Specimens for one sheet of 2219-T87 Aluminum Alloy

GENERAL DYNAMICS ASTRONAUTICS SAN DIEGO, CALIFORNIA	CODE IDENT NO. 05342	SIZE A	DRAWING NO. SPECIMEN LOCATION CHEM MILL & WELDED 2219 T87	PACKAGE NO.
	SCALE	RELEASED WE Wtz 3/3/76	SHEET	
		A2611 (11-62)	DISTR CODE	

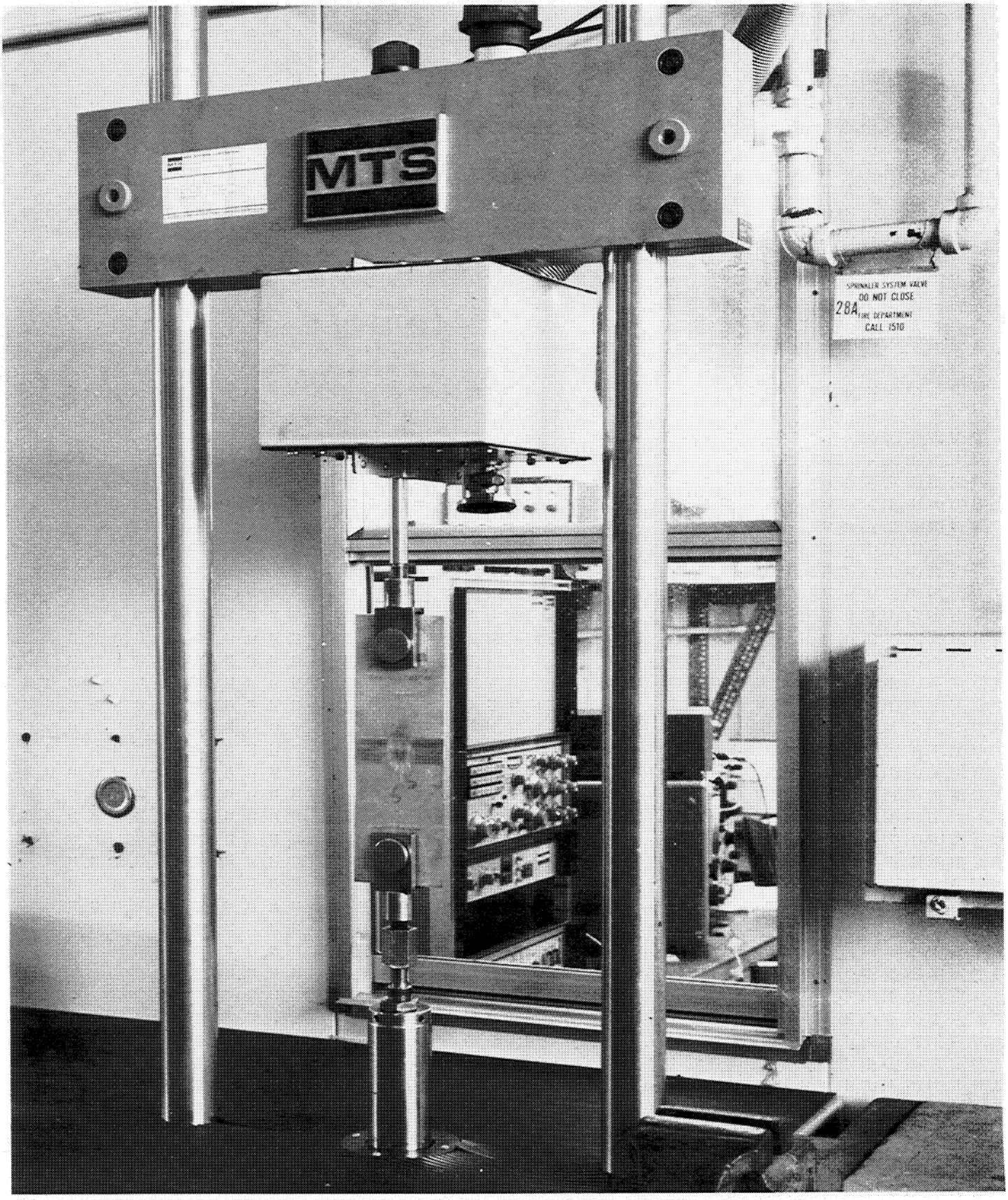

Figure 7. Center Notched Crack Propagation Specimen

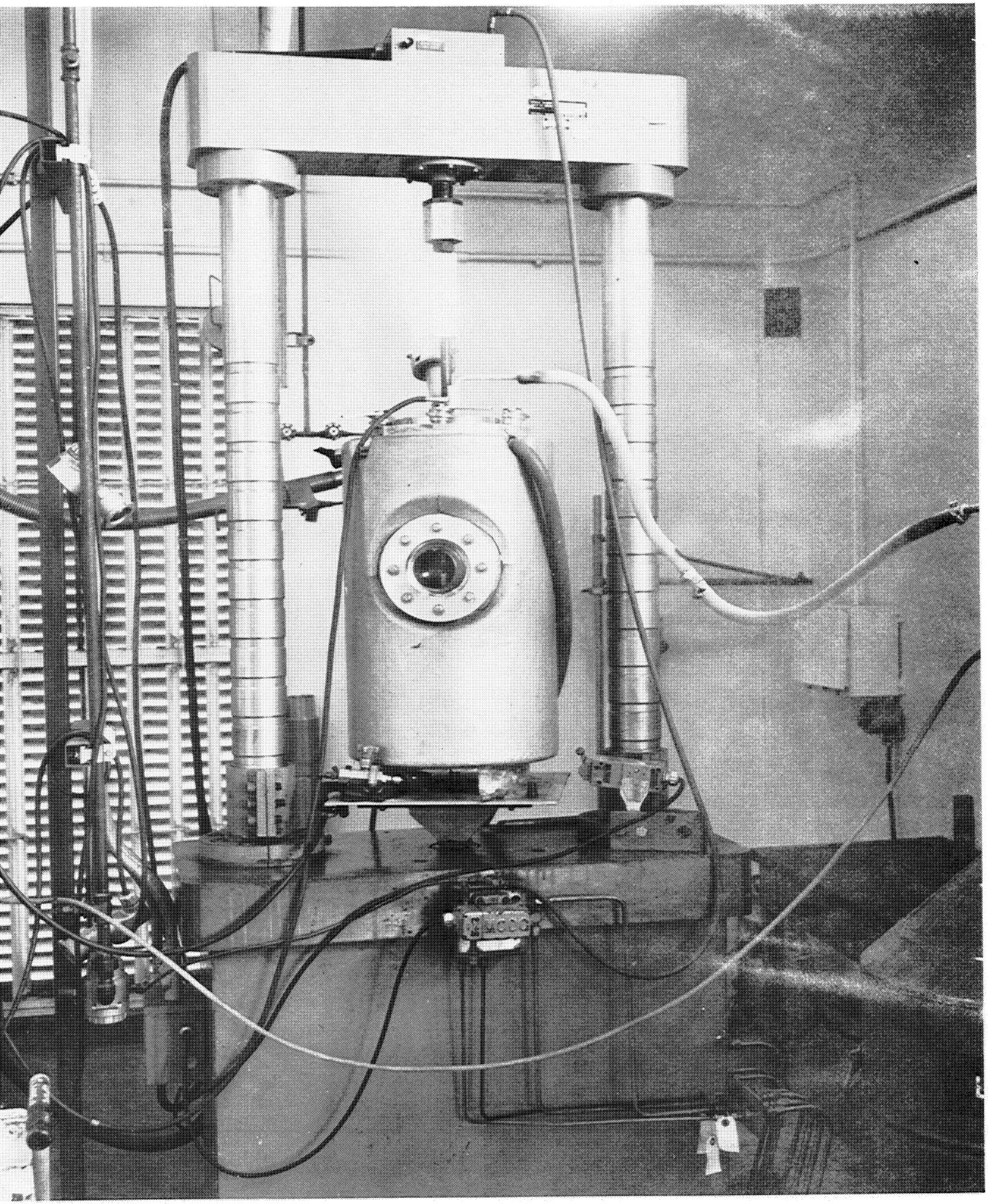

Figure 8. Viewing Liquid Hydrogen Cryostat in Tatnall Servo Controlled Test System

(Photo No. 15-3052)

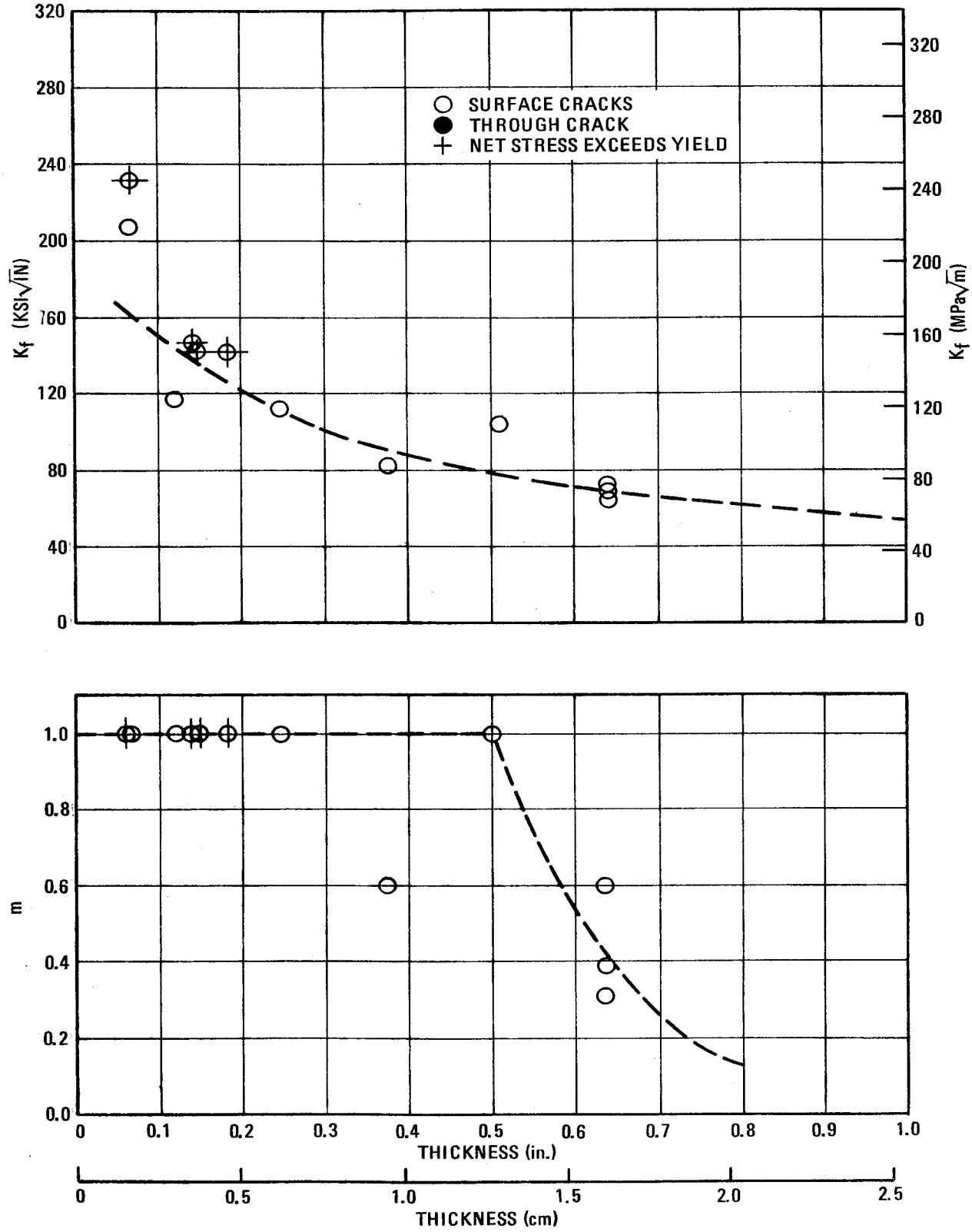

Figure 9. 2219-T87 LT-Direction (-320 F) (surface-cracks).

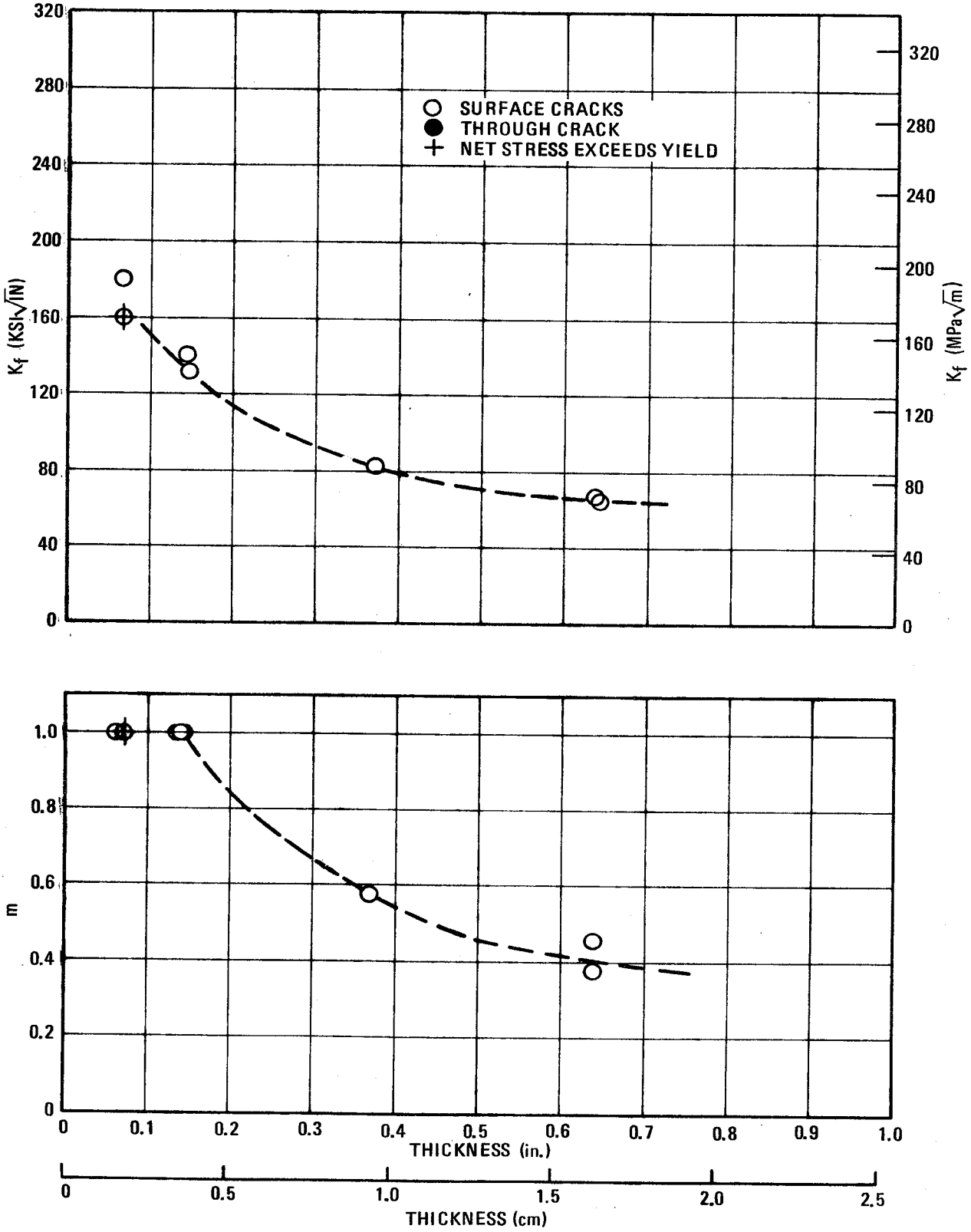

Figure 10. 2219-T87 LT-Direction (-423F) (surface cracks).

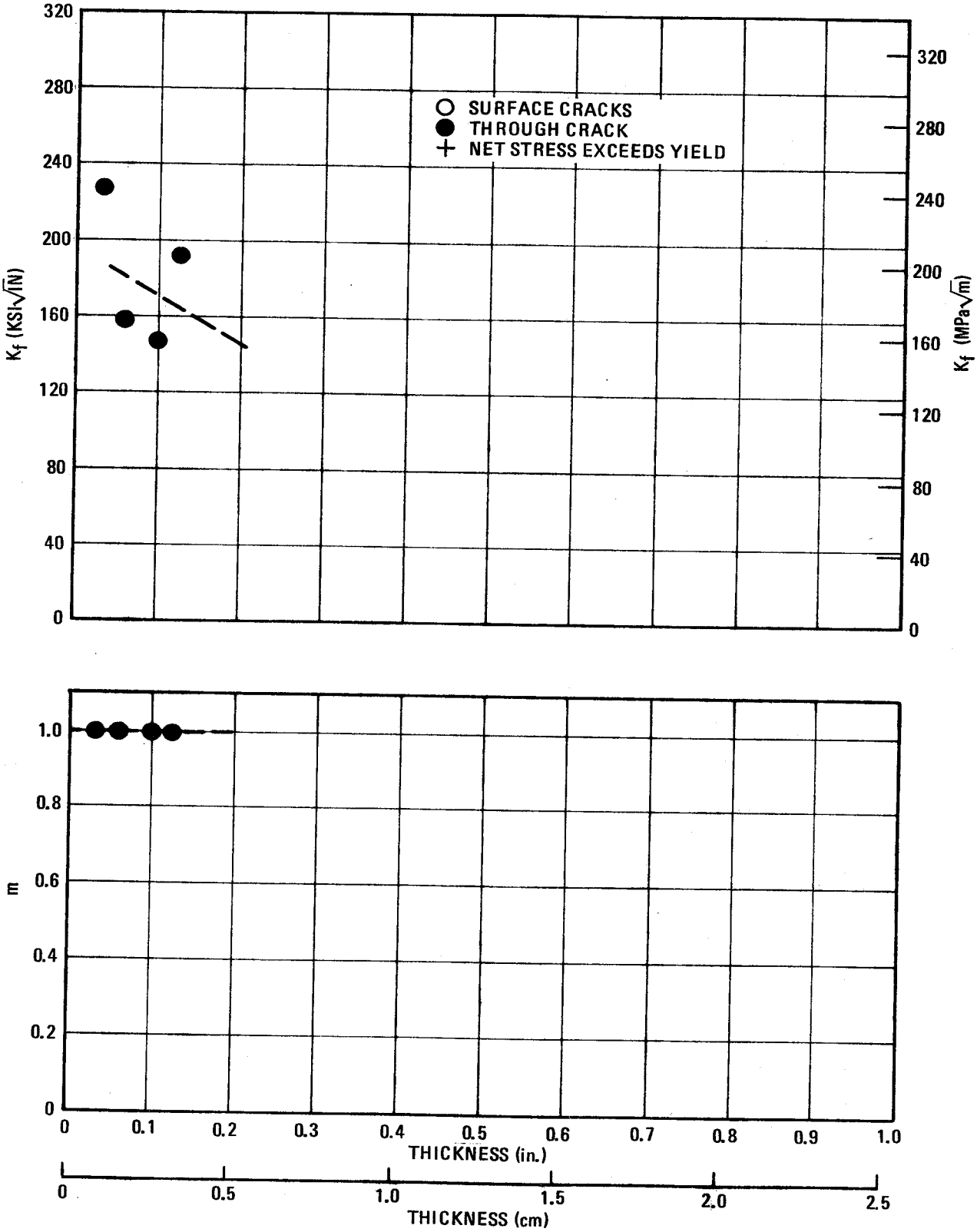

Figure 11. 2219-T87 TL-Direction (-423F) (through-cracks).

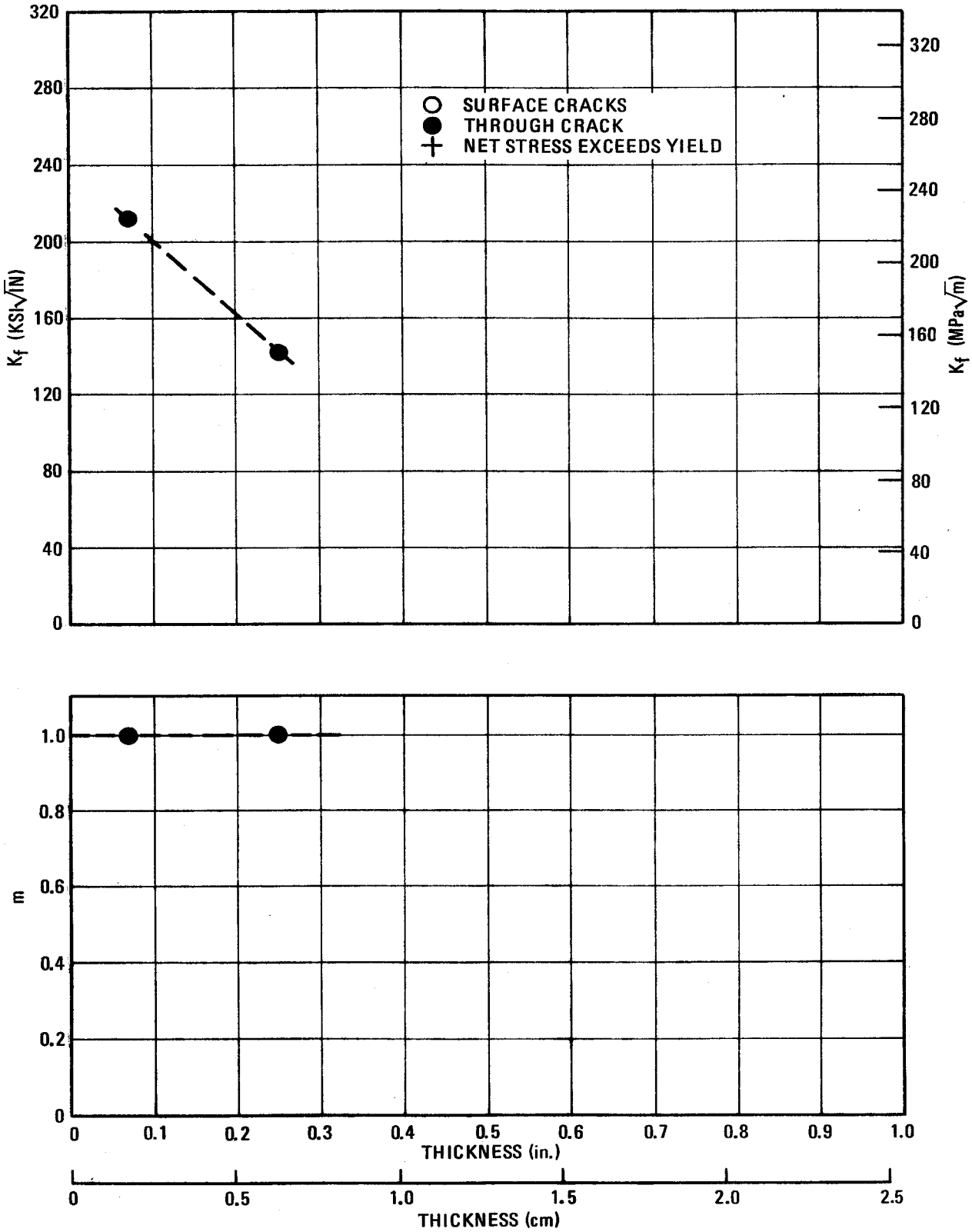

Figure 12. 2219-T87 LT-Direction (-423F) (through-cracks).

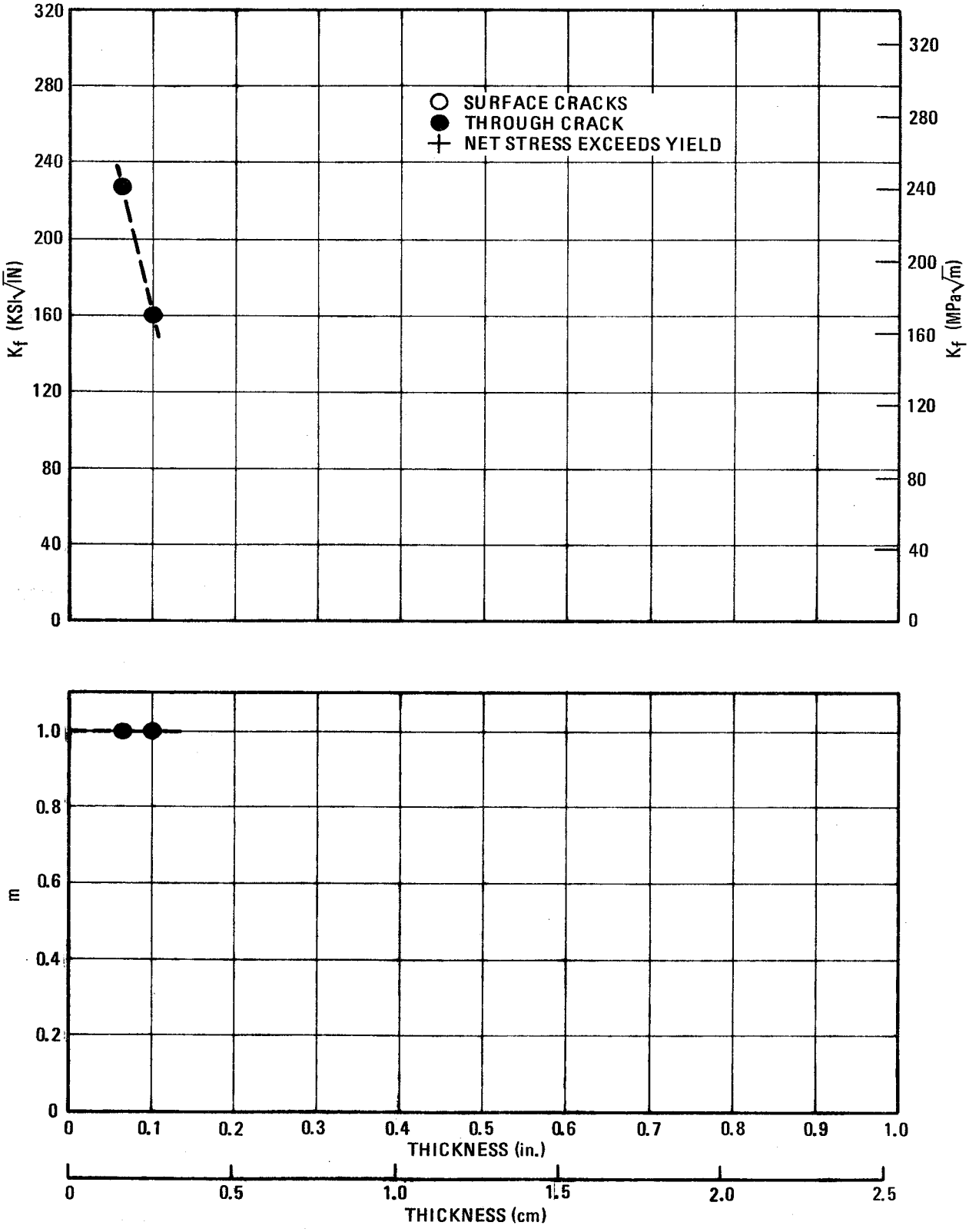

Figure 13. 2219-T87 TL-Direction (-320 F) (through-cracks).

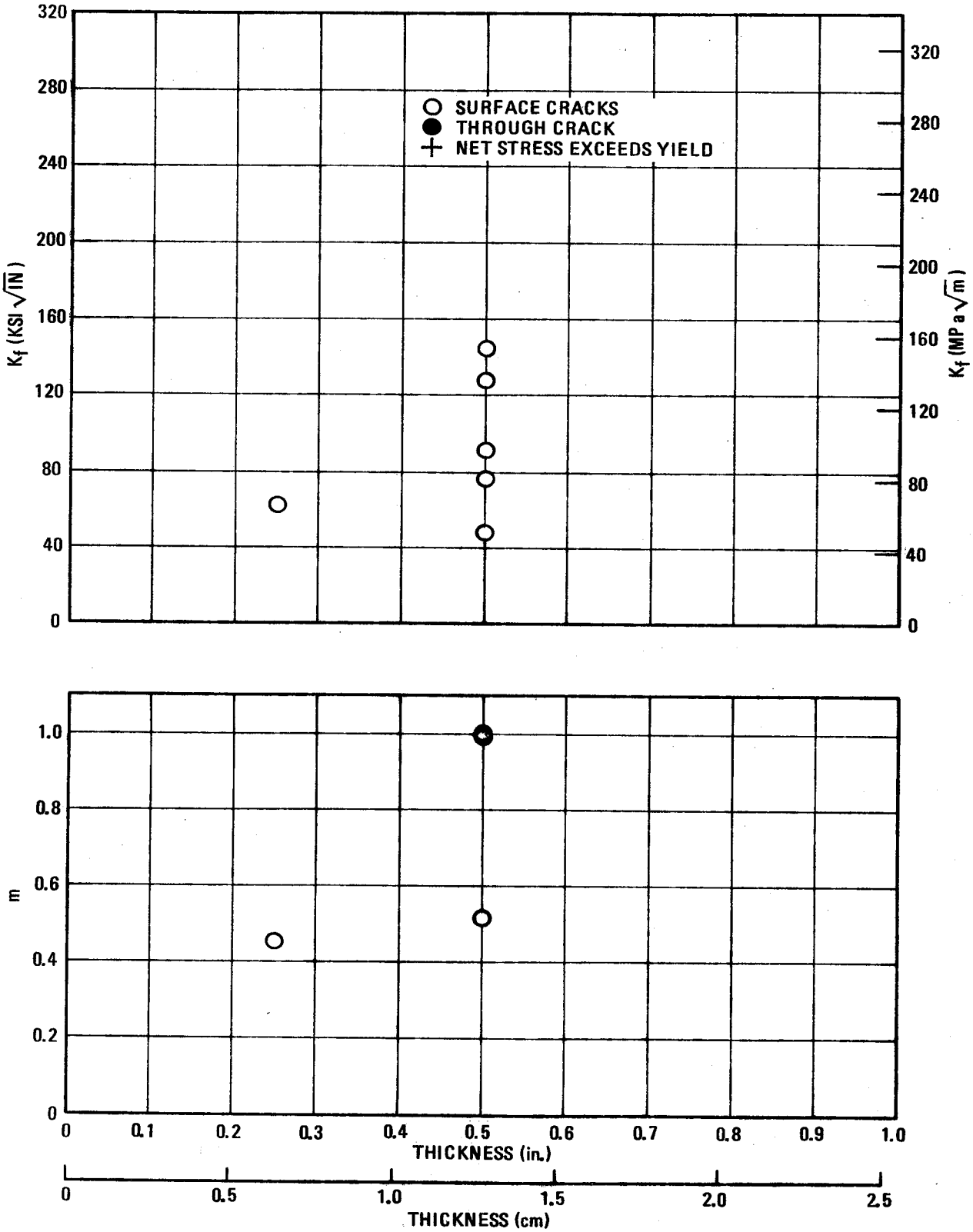

Figure 14. 2219-T87 TL-Direction (-320 F) (surface-cracks).

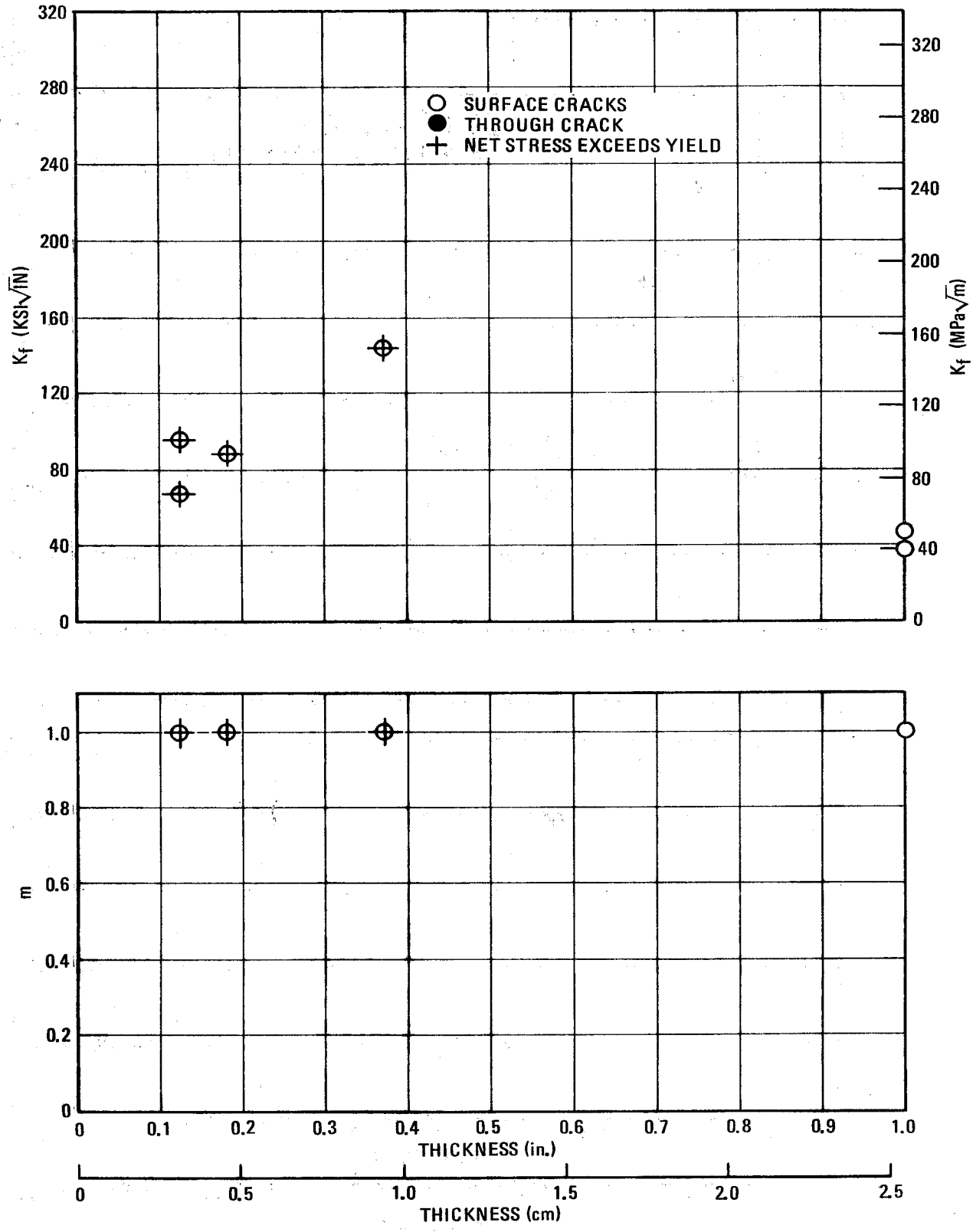

Figure 15. 2219-Weld (-423F) (surface-crack).

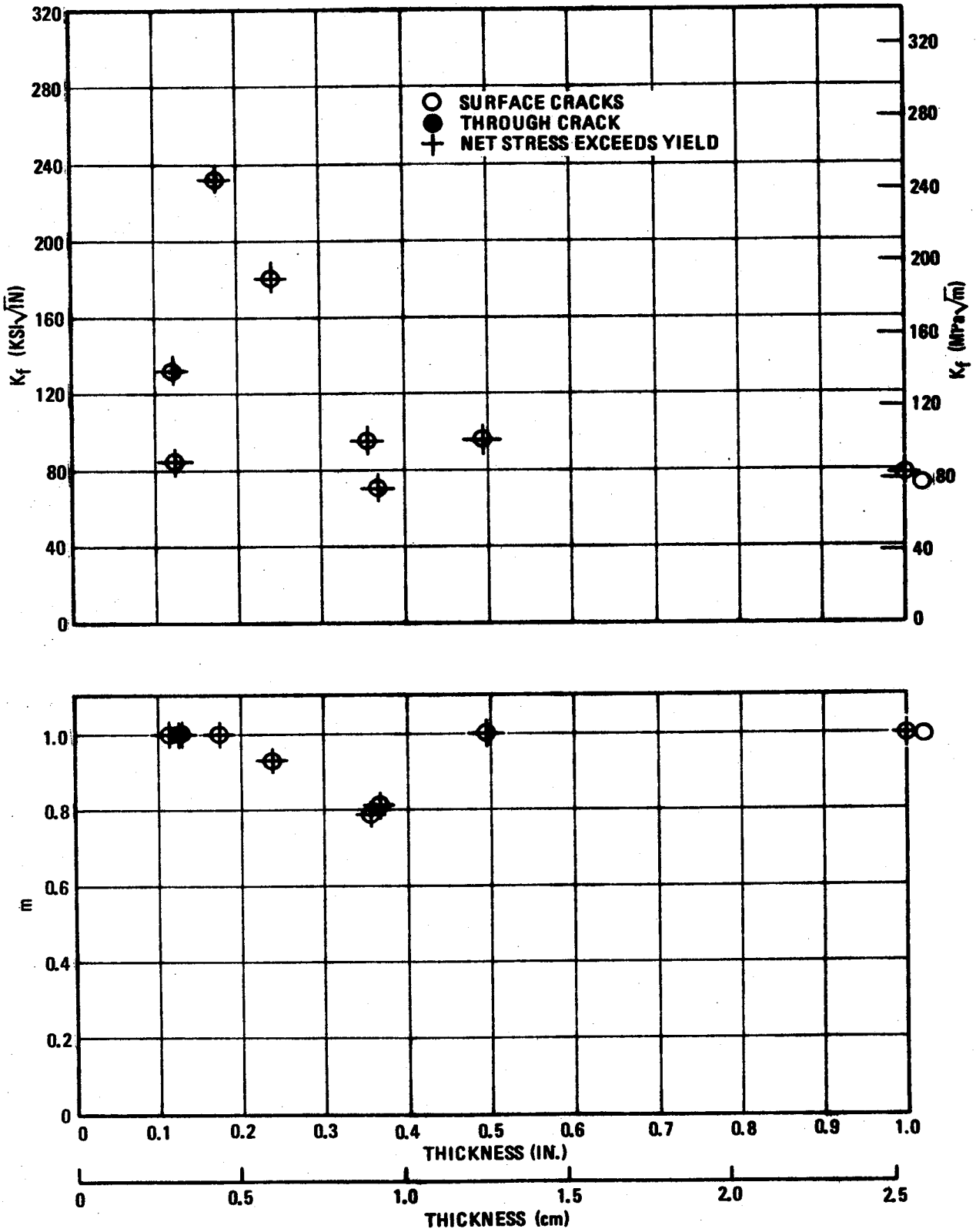

Figure 16. 2219-Weld (-320F) (surface-crack).

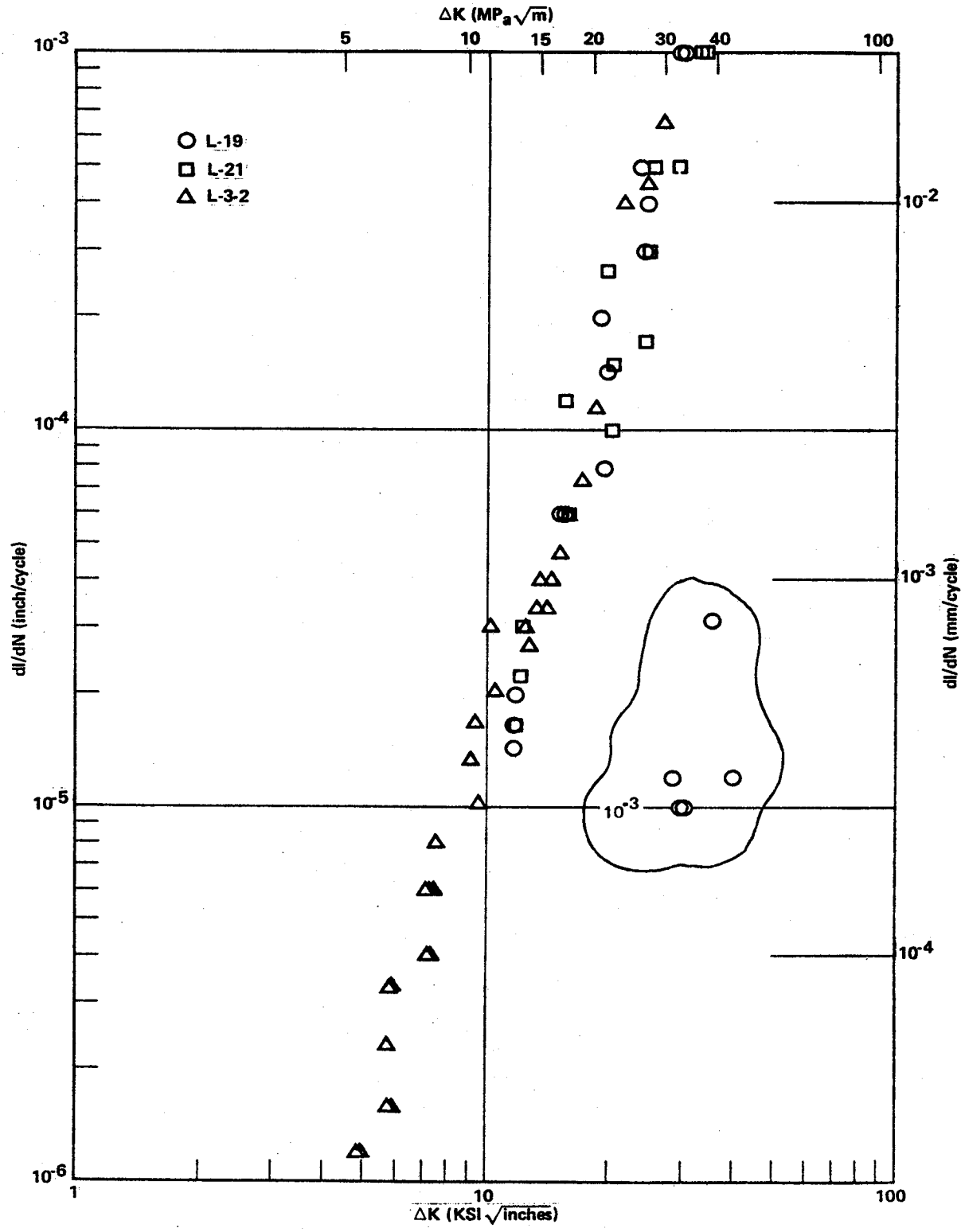

Figure 17. Crack Growth Rate for 2219-T87 Aluminum Alloy at Room Temperature (Specimens L-19, L-21, L-3-2)

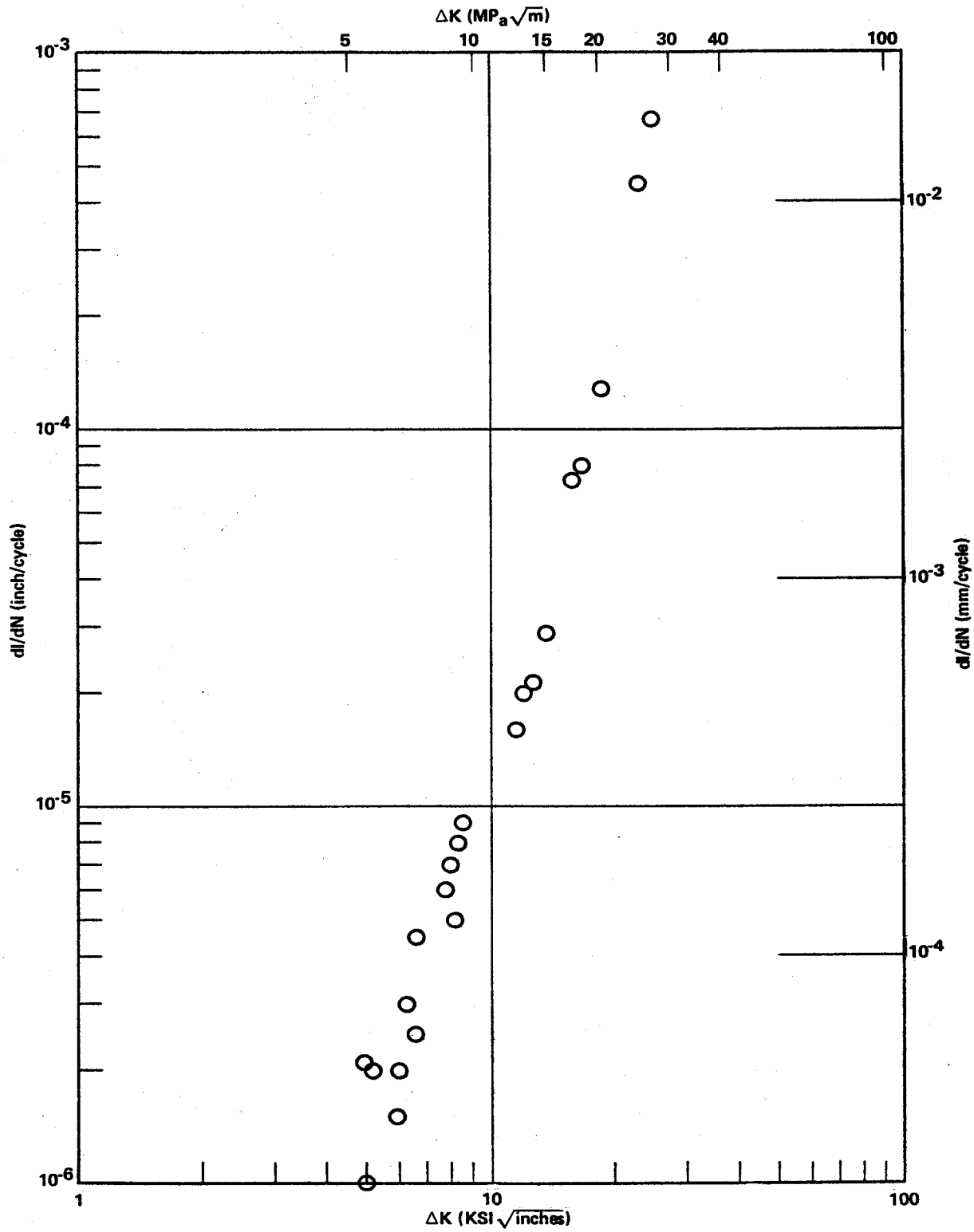

Figure 18. Crack Growth Rate for 2219-T87 Aluminum Alloy at Room Temperature (Specimen T12-3)

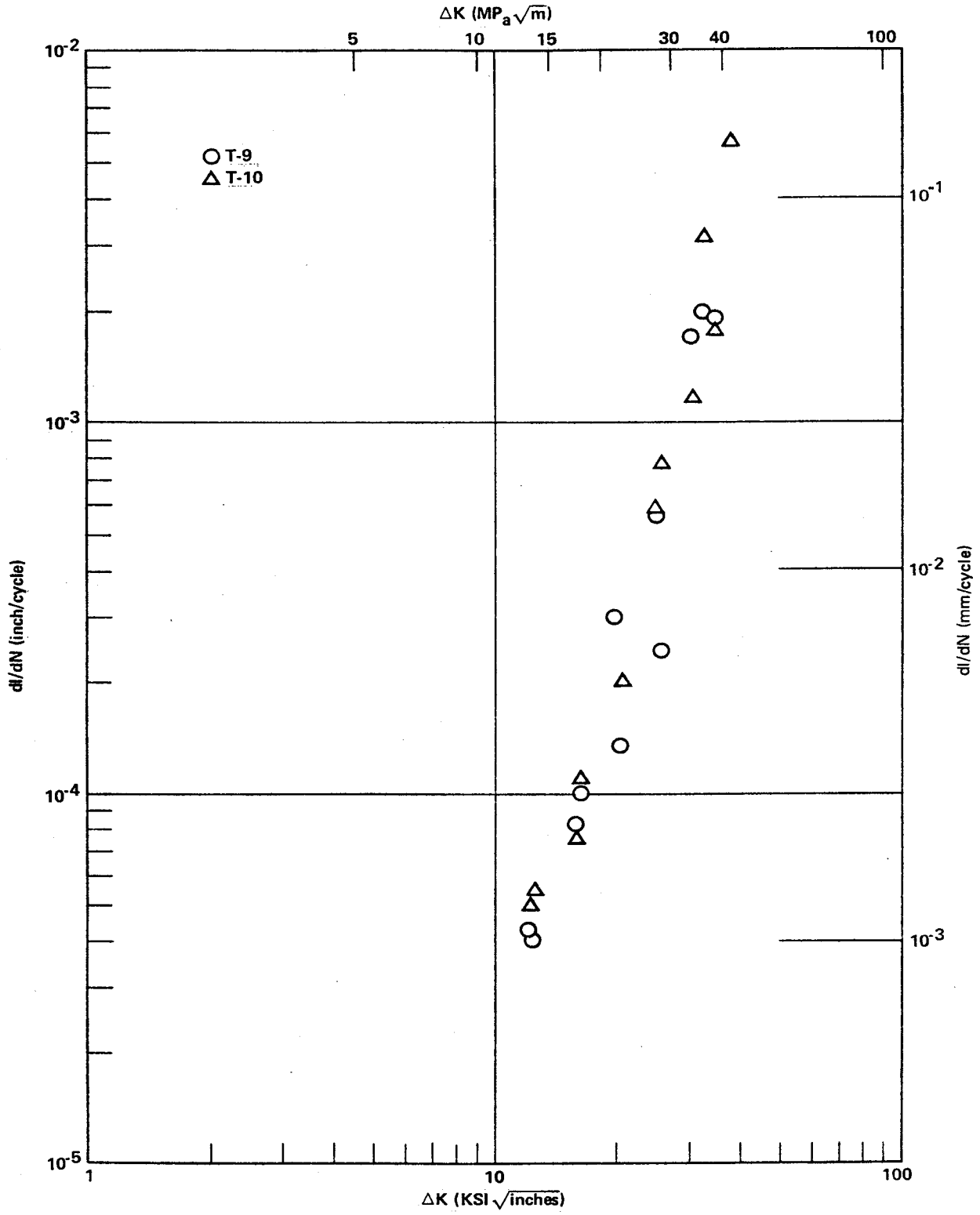

Figure 19. Crack Growth Rates for 2219-T87 Aluminum Alloy at Room Temperature (Specimens T9, T10)

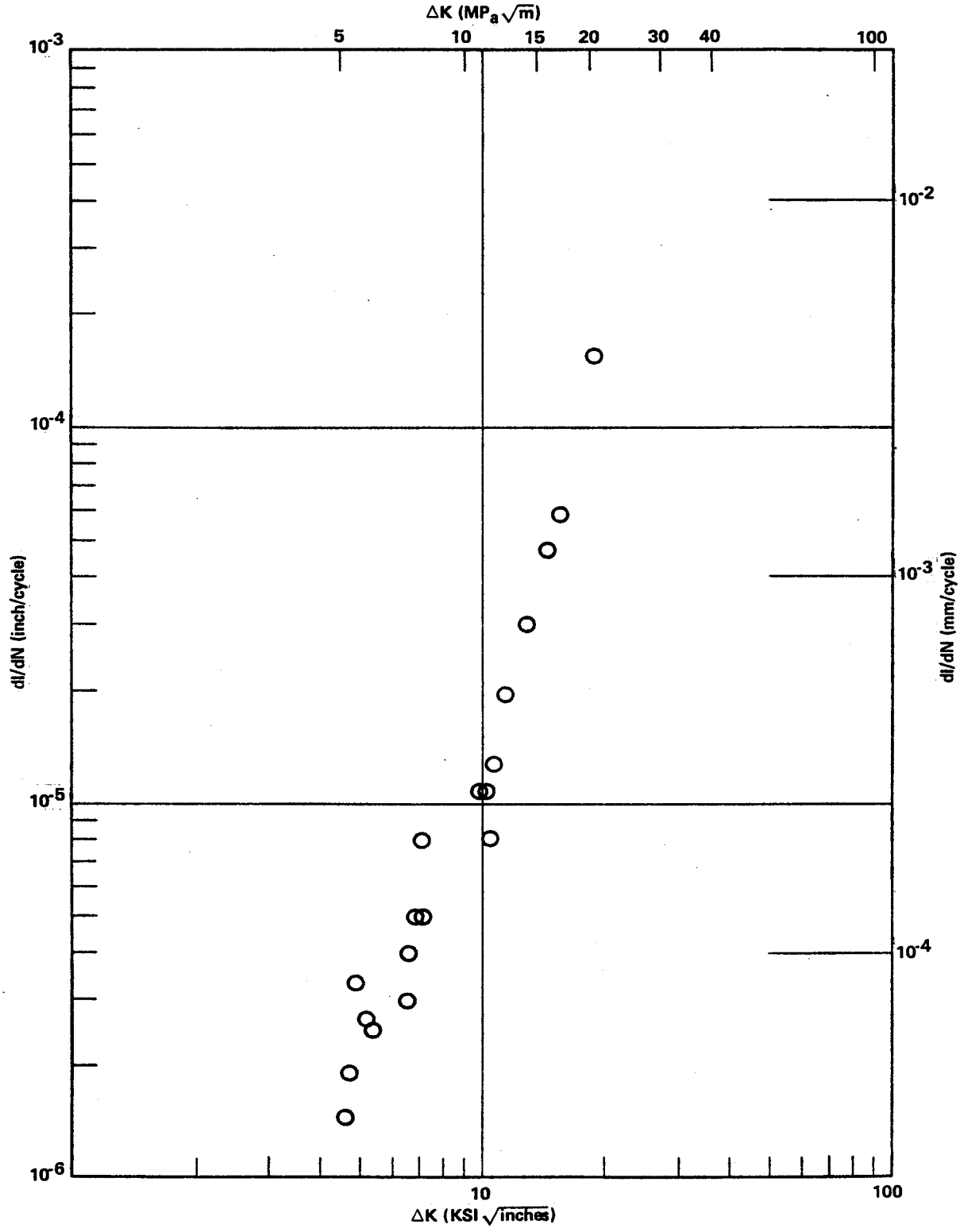

Figure 20. Crack Growth Rate for 2219 Aluminum Alloy Weldment at Room Temperature (Specimen W-11, thickness = 0.056")

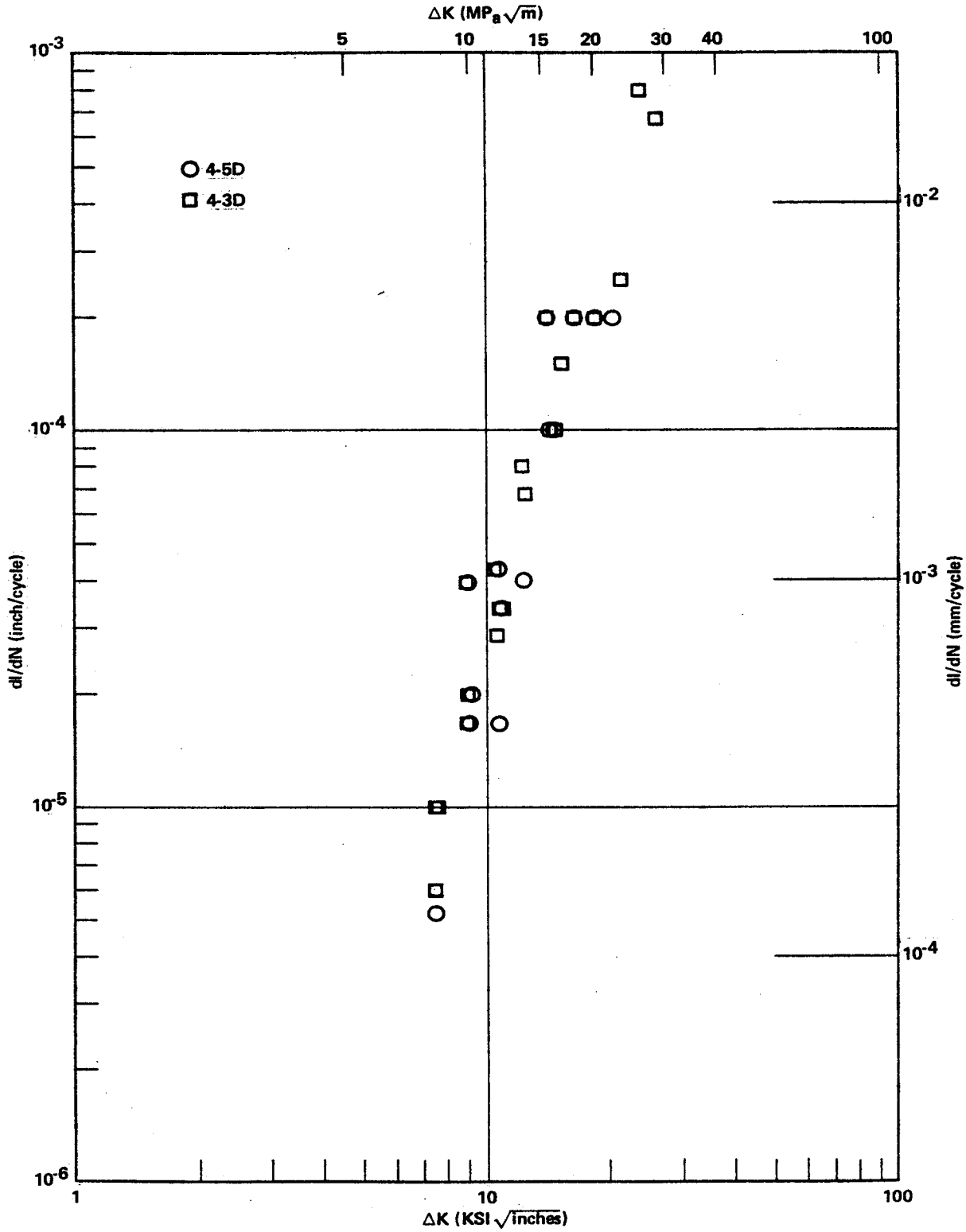

Figure 21. Crack Growth Rates for 2219 Aluminum Alloy Weldment at Room Temperature (Specimen 4-5D, 4-3D)

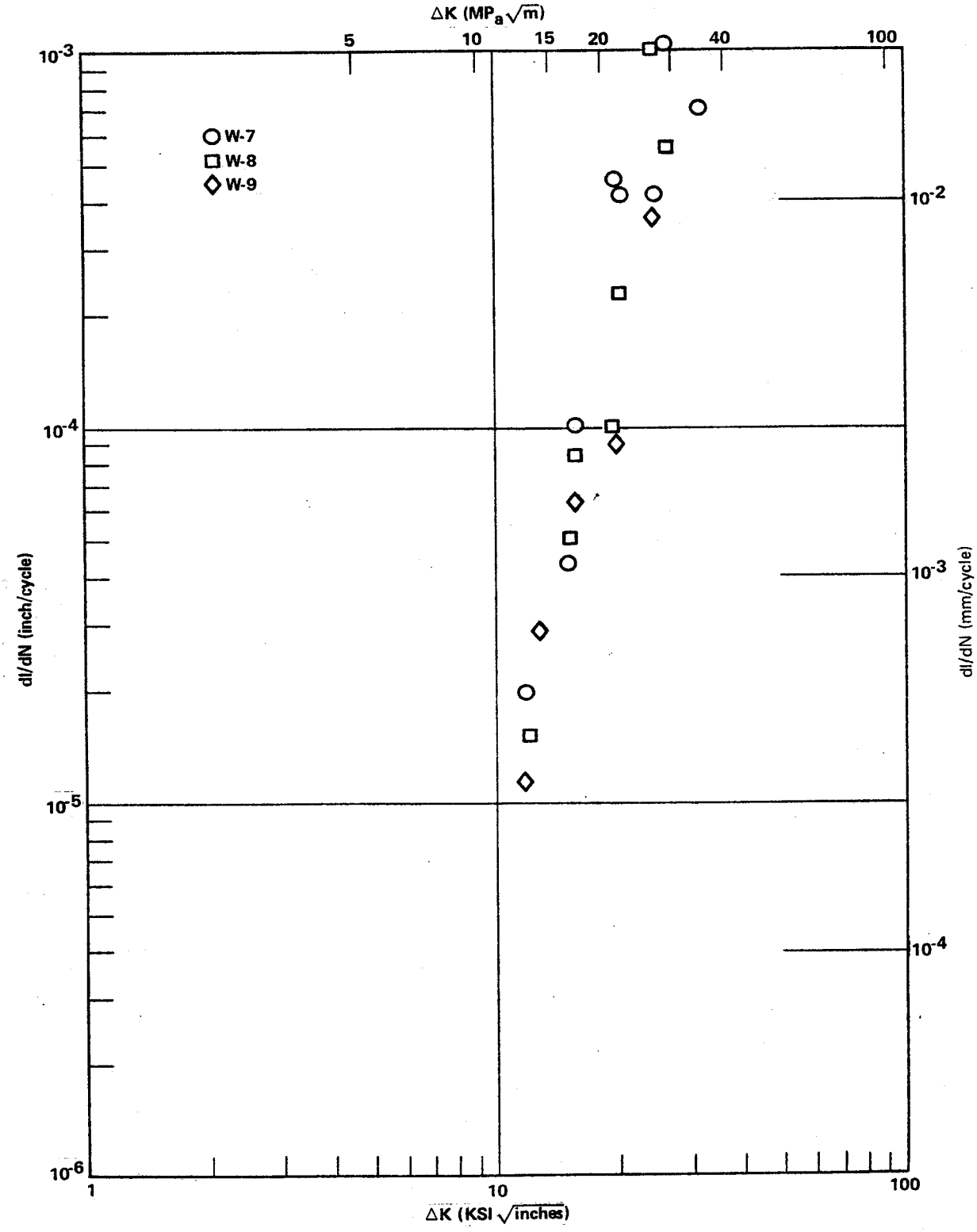

Figure 22. Crack Growth Rates for Welded 2219-T87 Aluminum Alloy at 20°K (Specimens W7, W8, W9)

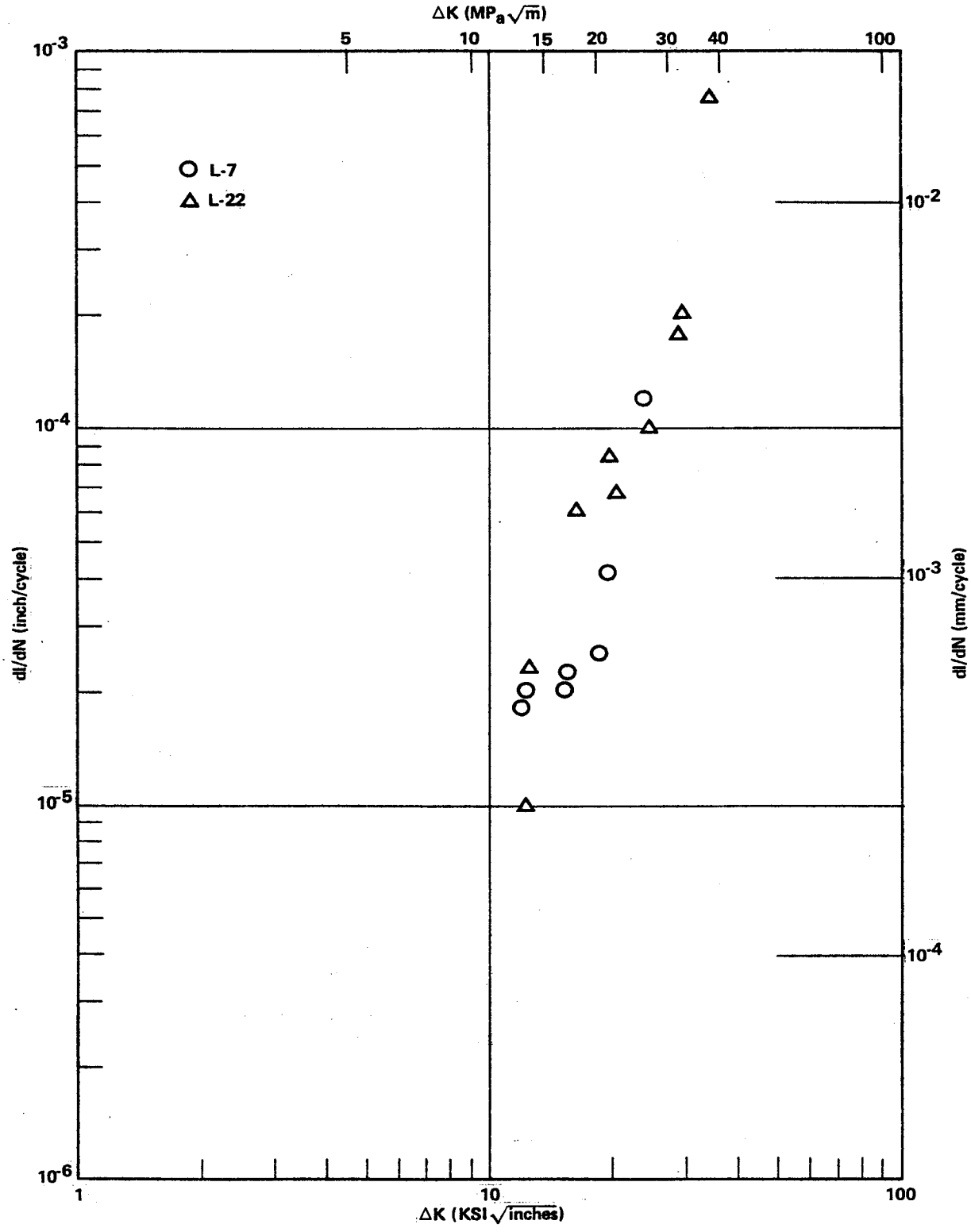

Figure 23. Crack Growth Rate for 2219-T87 Aluminum Alloy at 20°K (Specimens L-7, L-22)

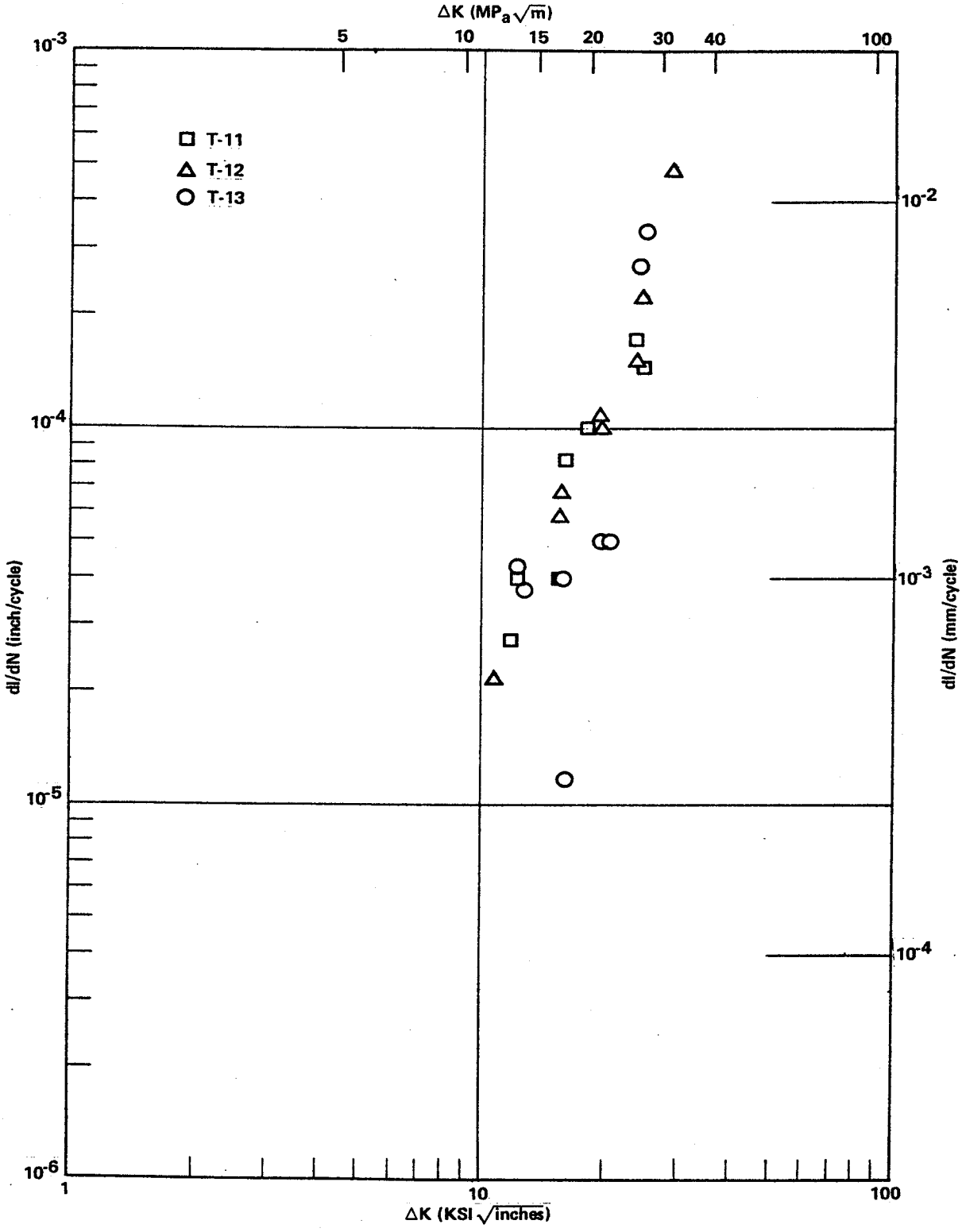

Figure 24. Crack Growth Rates for 2219-T87 Aluminum Alloy at 20°K (Specimens T11, T12, T13)

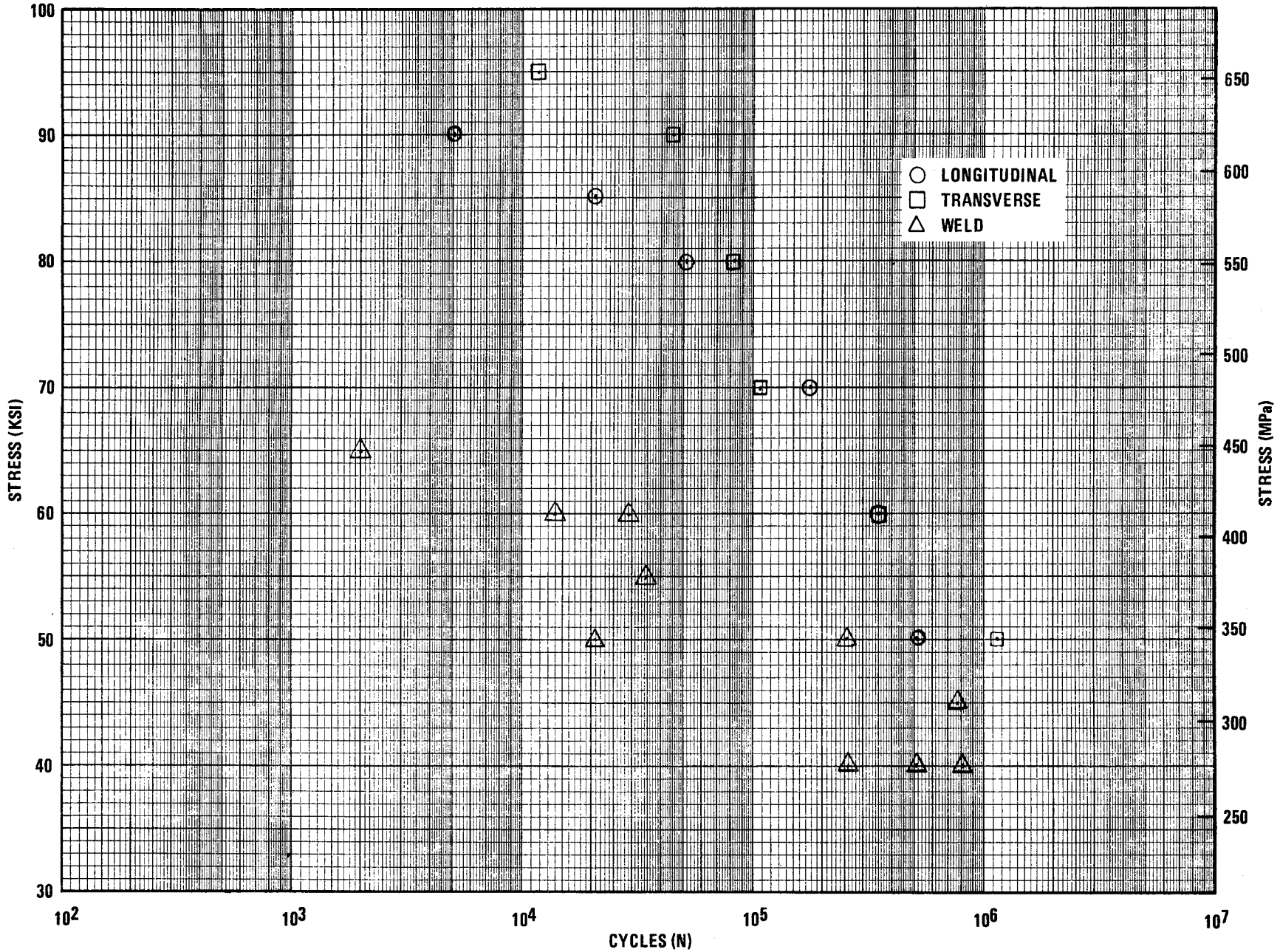

Figure 25. S-N Diagram for 2219-T87 Aluminum at 20° K.

Table 1. LH_2 Fuel Tank Sizing

Type I

Tank Material Density (Kg/m^3) =	2768
Est. Fwd. Sect. Thick. (cm) =	0.076
Est. Mid Sect. Thick. (cm) =	0.127
Est. Aft Sect. Thick.(cm) =	0.076
Insulation Density (Kg/m^3) =	49.55
Insulation Thick. (cm) =	6.5
Fluid Density (Kg/m^3) =	69.20

Tank Section	Fwd.	Mid	Aft	
Shell Type	Ellipsoid	Cylinder	Ellipsoid	Total
Length (cm)	215.5	396.4	215.5	827.5
Radius (cm)		304.8		
Volume (m^3)	41.93	115.71	41.93	199.58
Surf. Area (m^2)	47.38	75.93	47.38	170.68
Wt. of Shell (Kg)	338.41	649.10	338.41	1325.91
Wt. of Fluid (Kg)	2901.88	8006.94	2901.88	13810.69
Wt. of Total (Kg)	3240.29	8656.04	3240.29	15136.61
Shell Centroid (cm)	152.4	198.2	548.8	198.2
Fluid Centroid (cm)	114.3	198.2	510.7	198.2
Centroid Total (cm)	118.3	198.2	514.7	198.2

Type II

Tank Material Density (Kg/m^3) =	2768
Est. Fwd. Sect. Thick.(cm) =	0.051
Est. Mid Sect. Thick. (cm) =	0.102
Est. Aft Sect. Thick. (cm) =	0.051
Insulation Density (Kg/m^3) =	83.04
Insulation Thick. (cm) =	7.62
Fluid Density (Kg/m^3) =	69.20

Tank Section	Fwd.	Mid	Aft	
Shell Type	Hemisphere	Cylinder	Cone	Total
Length (cm)	203.2	1591.2	889.0	2683.4
Radius (cm)		203.2		
Volume (cm)	1576.2	18514	3448.0	23538,2
Surf. Area (m^2)	25.95	203.2	55.25	284.4
Wt. of Shell (Kg)	200.79	1858.13	427.60	2486.51
Wt. of Fluid (Kg)	1216.89	14293.30	2661.95	18174.41
Wt. of Total (Kg)	1417.68	16151.43	3089.54	20658.65
Shell Centroid (cm)	-101.6	795.6	1887.	910.9
Fluid Centroid (cm)	-76.2	795.6	1813.	886.3
Centroid Total (cm)	79.8	795.6	1823.	889.2

TABLE 2. LH_2 FUEL TANK STRESSES

DELTA PRES AT SL (kPa)	= 71.02	TANK MATERIAL	= 2219
DELTA PRES AT ALTITUDE (kPa)	= 123.14	FTY AT OPER TEMP (MPa)	= 455
BLOW-OUT PRES (kPa)	= 152.10	FTU AT OPER TEMP (MPa)	= 648
OPER PRES FACTOR	= 1.1	FTY AT RT (MPa)	= 351
LIN PRES FACTOR	= 1.33	FTU AT RT (MPa)	= 434
PROOF PRES FACTOR	= 1.03		
ULT PRES FACTOR	= 1.5		
BURST PRES FACTOR	= 2		
MAX MANEUVER FACTOR (LIM), NZ	= 2.5		
EMERG LAND FACTOR, NK	= -9		
AERO DRAG LIM LOAD (Kg)	= 0		
FLUID DENSITY (Kg/m^3)	= 69.20		
DIST TO FWD SUPPORT (cm)	= 0		
DIST TO AFT SUPPORT (cm)	= 346		

COND 1 - OPERATING PRESSURE

GAS PRES	NZ	NX	DRAG LOAD	R1	R2	ALLOW STRESS
135.48	0	0	0	0	0	455
POINT	1	2	3	4	5	6
THICK H	0.020	0.091	0.091	0.091	0.091	0.020
THICK L	0.051	0.046	0.046	0.046	0.046	0.051

COND 2 - LIMIT PRESSURE

GAS PRES	NZ	NX	DRAG LOAD	R1	R2	ALLOW STRESS
180.16	0	0	0	0	0	455
POINT	1	2	3	4	5	6
THICK H	0.028	0.122	0.122	0.122	0.122	0.128
THICK L	0.069	0.061	0.061	0.061	0.061	0.069

COND 3 - PROOF PRESSURE

GAS PRES	NZ	NX	DRAG LOAD	R1	R2	ALLOW STRESS
139.44	0	0	0	0	0	351
POINT	1	2	3	4	5	6
THICK H	0.028	0.122	0.122	0.122	0.122	0.028
THICK L	0.069	0.061	0.061	0.061	0.061	0.069

COND 4 - BURST PRESSURE

GAS PRES	NZ	NX	DRAG LOAD	R1	R2	ALLOW STRESS
270.90	0	0	0	0	0	648
POINT	1	2	3	4	5	6
THICK H	0.028	0.127	0.127	0.127	0.127	0.028
THICK L	0.071	0.064	0.064	0.064	0.064	0.071

Table 2 (continued)

COND 5 - 1G GROUND

GAS PRES	NZ	NX	DRAG LOAD	R1	R2	ALLOW STRESS
64.53	1.0	0	0			455
POINT	1	2	3	4	5	6
THICK H	0.010	0.046	0.043	0.046	0.046	0.010
THICK L	0.025	0.023	0.020	0.023	0.023	0.025

COND 6 - 1G FLIGHT

GAS PRES	NZ	NX	DRAG LOAD	R1	R2	ALLOW STRESS
135.48	1.0	0	0	16600	16600	455
POINT	1	2	3	4	5	6
THICK H	0.020	0.091	0.091	0.094	0.091	0.020
THICK L	0.051	0.046	0.046	0.046	0.046	0.051

COND 7 - 2G FLIGHT

GAS PRES	NZ	NX	DRAG LOAD	R1	R2	ALLOW STRESS
135.48	2.0	0	0	33200	33200	455
POINT	1	2	3	4	5	6
THICK H	0.020	0.094	0.091	0.097	0.094	0.097
THICK L	0.051	0.046	0.046	0.048	0.046	0.051

COND 8 - MAX MANEUVER

GAS PRES	NZ	NX	DRAG LOAD	R1	R2	ALLOW STRESS
203.19	3.75	0	0	62250	62250	648
POINT	1	23	3	4	5	6
THICK H	0.023	0.099	0.097	0.102	0.099	0.023
THICK L	0.053	0.051	0.048	0.051	0.051	0.051

COND 9 - EMERG LAND

GAS PRES	NZ	NX	DRAG LOAD	R1	R2	ALLOW STRESS
78.12	0	-0.0	0	229728	-229728	648
POINT	1	2	3	4	5	6
THICK H	0.013	0.053	0.048	0.048	0.043	0.010
THICK L	0.033	0.028	0.015	0.036	0.020	0.023

COND 10 - COMPARTMENT BLOW-OUT

GAS PRES	NZ	NX	DRAG LOAD	R1	R2	ALLOW STRESS
173.41	2.50	0	0	41500	41500	455
POINT	1	2	3	4	5	6
THICK H	0.025	0.119	0.117	0.122	0.119	0.025
THICK L	0.066	0.061	0.058	0.061	0.061	0.066
REQUIRED T	0.071	0.127	0.127	0.127	0.127	0.071

Table 2 (continued)

COND 1 - OPERATING PRESSURE

GAS PRES	NZ	NX	DRAG LOAD	R1	R2	
135.48	0	0	0	0	0	
POINT	1	2	3	4	5	6
STRESS H	129	324	324	324	324	129
STRESS L	324	162	162	162	162	324

COND 2 - LIMIT PRESSURE

GAS PRES	NZ	NX	DRAG LOAD	R1	R2	
180.16	0	0	0	0	0	
POINT	1	2	3	4	5	6
STRESS H	172	431	431	431	431	172
STRESS L	431	215	215	215	215	431

COND 3 - PROOF PRESSURE

GAS PRES	NZ	NX	DRAG LOAD	R1	R2	
139.55	0	0	0	0	0	
POINT	1	2	3	4	5	6
STRESS H	133	334	334	334	334	133
STRESS L	334	167	167	167	167	334

COND 4 - BURST PRESSURE

GAS PRES	NZ	NX	DRAG LOAD	R1	R2	
370.90	0	0	0	0	0	
POINT	1	2	3	4	5	6
STRESS H	259	648	648	648	648	259
STRESS L	648	324	324	324	324	648

COND 5 - 1G GROUND

GAS PRES	NZ	NX	DRAG LOAD	R1	R2	
64.53	1.0	0	0	16600	16600	
POINT	1	2	3	4	5	6
STRESS H	62.7	159	154	164	159	62.7
STRESS L	157	79.7	77.1	82.3	79.7	157

COND 6 - 1G FLIGHT

GAS PRES	NZ	NX	DRAG LOAD	R1	R2	
135.48	1.0	0	0	16600	16600	
POINT	1	2	3	4	5	6
STRESS H	75.4	329	324	334	329	131
STRESS L	326	165	162	167	164	327

TABLE 2 (continued)

COND 7 - 2G FLIGHT

GAS PRES	NZ	NX	DRAG LOAD	R1	R2	
135.48	2.0	0	0	33200	33200	
POINT	1	2	3	4	5	6
STRESS H	132	334	324	344	334	132
STRESS L	329	167	162	172	167	329

COND 8 - MAX MANEUVER

GAS PRES	NZ	NX	DRAG LOAD	R1	R2	
203.19	3.75	0	0	62250	62250	
POINT	1	2	3	4	5	6
STRESS H	198	505	486	523	505	198
STRESS L	495	252	242	262	252	495

COND 9 - EMERG LAND

GAS PRES	NZ	NX	DRAG LOAD	R1	R2	
78.12	0	-9.0	0	229728	-229728	
POINT	1	2	3	4	5	6
STRESS H	117	276	247	247	218	81.0
STRESS L	292	138	75.0	184	109	203

COND 10 - COMPARTMENT BLOW-OUT

GAS PRES	NZ	NX	DRAG LOAD	R1	R2	
173.40	2.5	0	0	41500	41500	
POINT	1	2	3	4	5	6
STRESS H	168	427	415	440	427	168
STRESS L	421	214	207	220	214	421

Table 3. Stress Spectrum for LH_2 Fuel Tank - Type I

Segment	Temperature	Occurrences			Analysis Pt. 3H		
		Flight	Block	Life	S_{mean} (MPa)	S_{max} (MPa)	S_{min} (MPa)
Proof Test	RT	.001	1.0	50	166.9	333.8	0
Leak Test	RT	.01	10.0	500	77.22	154.4	0
1 G Ground	LH_2				154.4	-	-
Taxi $\Delta g \geq .3$	LH_2	1.600	1600	80000	154.4	154.4	154.4
1 G Flight	LH_2				324.1	-	-
2 G Flight	LH_2				324.1	-	-
Man. $.5 > \Delta g \geq .3$	LH_2	1.902	1902	95100	324.1	324.1	324.1
Man. $\Delta g \geq .5$	LH_2	.040	40	2000	324.1	324.1	324.1
Gust $.5 > \Delta g \geq .3$	LH_2	3.315	3315	165750	324.1	324.1	324.1
Gust $\Delta g \geq .5$	LH_2	.429	429	21450	324.1	324.1	324.1
G-A-G	LH_2				239.2	324.1	154.4

Table 4. TENSILE PROPERTIES, FRACTURE CONSTANTS, AND TEST CONDITIONS FOR SURFACE- AND THROUGH-FLAW DATA. SI UNITS (U.S. CUSTOMARY UNITS)

MATERIAL & FLAW ORIENTATION		TEST TEMPERATURE °K	°F	NOMINAL THICKNESS MM	IN	ULTIMATE STRESS MN/m²	KSI	YIELD STRESS MN/m²	KSI	K_f MN/m$^{3/2}$	KSI√IN	M	REF., PAGE
2219-T87					(SURFACE FLAW)								
LT		20	-423	3.61	.142	662.1	96.0	482.8	70.0	147.3	133.8	1.00	4, 63
LT		20	-423	3.58	.141	662.1	96.0	482.8	70.0	155.4	141.4	1.00	4, 65
LT		20	-423	9.37	.369	662.1	96.0	482.8	70.0	89.8	81.7	.59	4, 66
LT		20	-423	16.23	.639	640.7	92.9	493.1	71.5	72.0	65.5	.36	6, 99
LT		20	-423	16.15	.636	640.7	92.9	493.1	71.5	73.1	66.5	.46	8, 100
LT		20	-423	1.68	.066	655.9	95.1	485.5	70.4	186.6	169.8	1.00	8, 102
LT	*	20	-423	1.70	.067	655.9	95.1	485.5	70.4	174.7	159.0	1.00	8, 103
2219-T87					(SURFACE FLAW)								
LT		77	-320	3.10	.122	604.8	87.7	441.4	64.0	129.3	117.4	1.00	4, 63
LT	*	77	-320	3.61	.142	604.8	87.7	441.4	64.0	150.3	136.8	1.00	4, 64
LT	*	77	-320	3.69	.145	604.8	87.7	441.4	64.0	155.6	141.6	1.00	4, 65
LT	*	77	-320	4.65	.183	604.8	87.7	441.4	64.0	154.8	140.9	1.00	4, 66
LT		77	-320	6.27	.247	604.8	87.7	441.4	64.0	123.5	112.4	1.00	4, 67
LT		77	-320	9.47	.373	604.8	87.7	441.4	64.0	90.1	82.0	.60	4, 68
LT		77	-320	16.21	.638	569.7	85.5	462.8	67.1	75.5	68.7	.31	6, 98
LT		77	-320	16.15	.636	589.7	85.5	462.8	67.1	69.5	63.2	.39	8, 96
LT		77	-320	16.15	.636	589.7	85.5	462.8	67.1	79.1	72.0	.66	8, 99
LT		77	-320	1.70	.067	560.7	81.3	441.4	64.0	227.9	207.4	1.00	8, 101
LT	*	77	-320	1.68	.066	560.7	81.3	441.4	64.0	257.3	234.1	1.00	8, 102
LT		77	-320	12.89	.507	577.9	83.8	454.5	65.9	113.7	103.5	1.00	9, 185
2219-T87					(SURFACE FLAW)								
LT	*	294	70	3.10	.122	441.4	64.0	365.5	53.0	144.5	131.5	.96	4, 63
LT	*	294	70	3.63	.143	441.4	64.0	365.5	53.0	227.1	206.6	1.00	4, 64
LT	*	294	70	3.66	.144	441.4	64.0	365.5	53.0	317.9	289.3	1.00	4, 65
LT	*	294	70	4.65	.183	441.4	64.0	365.5	53.0	247.6	225.3	1.00	4, 66
LT		294	70	6.27	.247	441.4	64.0	365.5	53.0	175.0	159.2	1.00	4, 67
LT	*	294	70	9.47	.373	441.4	64.0	365.5	53.0	89.8	81.7	.58	4, 68
LT	*	294	70	16.08	.633	477.9	69.3	386.2	56.0	84.7	77.1	.63	8, 97
LT	*	294	70	16.26	.640	477.9	69.3	386.2	56.0	71.1	64.7	.53	6, 97
LT		294	70	1.68	.066	469.0	68.0	384.8	55.8	205.4	186.9	1.00	8, 100
LT	*	294	70	1.68	.066	469.0	68.0	384.8	55.8	92.3	84.0	.74	8, 101
LT		294	70	16.41	.646	473.8	68.7	391.0	56.7	77.3	70.3	.62	9, 180
LT		294	70	12.70	.500	475.9	69.0	387.6	56.2	123.5	112.4	1.00	9, 184
2219-T87					(SURFACE FLAW)								
LT	*	394	250	3.10	.122	377.2	54.7	324.1	47.0	150.5	137.2	.66	4, 63
LT	*	394	250	3.63	.143	377.2	54.7	324.1	47.0	727.3	661.5	.99	4, 65
LT	*	394	250	6.27	.247	377.2	54.7	324.1	47.0	325.1	295.9	1.00	4, 67
LT	*	449	350	3.10	.122	311.0	45.1	275.9	40.0	75.7	68.9	.63	4, 63

Table 5. TENSILE PROPERTIES, FRACTURE CONSTANTS, AND TEST CONDITIONS FOR SURFACE- AND THROUGH-FLAW DATA. SI UNITS (U.S. CUSTOMARY UNITS)

MATERIAL & FLAW ORIENTATION		TEST TEMPERATURE °K	°F	NOMINAL THICKNESS MM	IN	ULTIMATE STRESS MN/m²	KSI	YIELD STRESS MN/m²	KSI	K_f MN/m$^{3/2}$	KSI√IN	M	REF., PAGE
2219-T87						(SURFACE FLAW)							
TL		77	-320	12.70	.500	584.8	84.8	454.5	65.9	138.9	126.4	.96	9, 186
TL		77	-320	12.73	.501	584.8	84.8	454.5	65.9	157.3	143.1	1.00	9, 186
TL		77	-320	12.67	.499	584.8	84.8	454.5	65.9	82.2	74.8	.53	9, 186
TL		77	-320	12.70	.500	584.8	84.8	454.5	65.9	52.4	47.7	-.14	9, 186
TL		77	-320	12.70	.500	584.8	84.8	454.5	65.9	99.6	90.6	1.00	9, 187
TL		77	-320	6.35	.250	584.8	84.8	454.5	65.9	67.5	61.4	.45	9, 187
TL		144	-200	6.27	.247	524.8	76.1	424.8	61.6	52.6	47.9	.50	7, 121
TL	*	144	-200	3.18	.125	524.8	76.1	424.8	61.6	43.2	39.3	.50	7, 121
TL	*	291	65	6.27	.247	468.3	67.9	380.7	55.2	215.2	195.8	1.00	7, 121
TL	*	291	65	3.28	.129	468.3	67.9	380.7	55.2	21.9	19.9	0.00	7, 121
TL		294	70	6.35	.250	475.9	69.0	387.6	56.2	77.4	70.4	.67	9, 184
TL	*	449	350	6.27	.247	326.9	47.4	291.0	42.2	177.7	161.7	1.00	7, 121

* Net stress exceeds yield stress

** Net stress exceeds ultimate stress

Table 6. TENSILE PROPERTIES, FRACTURE CONSTANTS, AND TEST CONDITIONS FOR SURFACE- AND THROUGH-FLAW DATA. SI UNITS (U.S. CUSTOMARY UNITS)

MATERIAL & FLAW ORIENTATION		TEST TEMPERATURE °K	°F	NOMINAL THICKNESS MM	IN	ULTIMATE STRESS MN/m^2	KSI	YIELD STRESS MN/m^2	KSI	K_f $MN/m^{3/2}$	KSI/IN	M	REF., PAGE
2219-T87						(THROUGH FLAW)							
LT		20	-423	1.73	.068	664.1	96.3	487.6	70.7	232.2	211.3	1.00	6, TABLE 3
LT		20	-423	6.35	.250	684.8	99.3	497.9	72.2	156.7	142.6	1.00	9, 228
LT	*	77	-320	1.73	.068	466.9	67.7	379.3	55.0	290.4	264.2	1.00	6, TABLE 3
LT	*	294	70	1.73	.068	466.9	67.7	379.3	55.0	286.6	260.9	1.00	6, TABLE 3
LT		294	70	2.54	.100	473.8	68.7	391.0	56.7	223.2	203.1	.83	9, 227

* Net stress exceeds yeild stress

** Net stress exceeds ultimate stress

Table 7. TENSILE PROPERTIES, FRACTURE CONSTANTS, AND TEST CONDITIONS FOR SURFACE- AND THROUGH-FLAW DATA. ST UNITS (U.S. CUSTOMARY UNITS)

MATERIAL & FLAW ORIENTATION	TEST TEMPERATURE °K	°F	NOMINAL THICKNESS MM	IN	ULTIMATE STRESS MN/m^2	KSI	YIELD STRESS MN/m^2	KSI	K_f $MN/m^{3/2}$	KSI√IN	M	REF., PAGE
2219-T87					(THROUGH FLAW)							
TL	20	-423	.81	.032	692.4	100.4	495.2	71.8	250.8	228.2	1.00	9, 228
TL	20	-423	1.55	.061	692.4	100.4	495.2	71.8	174.3	158.6	1.00	9, 228
TL	20	-423	3.18	.125	692.4	100.4	495.2	71.8	211.2	192.2	.96	9, 228
TL	20	-423	2.54	.100	692.4	100.4	495.2	71.8	161.4	146.9	1.00	9, 226
TL	77	-321	1.57	.062	584.8	84.8	454.5	65.9	250.2	227.7	1.00	9, 228
TL	77	-321	2.54	.100	584.8	84.8	454.5	65.9	175.4	159.6	1.00	9, 228
TL	294	70	1.57	.062	475.9	69.0	387.6	56.2	14.9	13.6	-3.85	9, 227

* Net stress exceeds yield stress

** Net stress exceeds ultimate stress

Table 8. TENSILE PROPERTIES, FRACTURE CONSTANTS, AND TEST CONDITIONS FOR SURFACE- AND THROUGH-FLAW DATA. SI UNITS (U.S. CUSTOMARY UNITS)

MATERIAL & FLAW ORIENTATION		TEST TEMPERATURE °K	°F	NOMINAL THICKNESS MM	IN	ULTIMATE STRESS MN/m²	KSI	YIELD STRESS MN/m²	KSI	K_f MN/m$^{3/2}$	KSI√IN	M	REF., PAGE
2219-WELD						(SURFACE FLAW)							
	*	20	-423	4.65	.183	365.5	53.0	165.5	24.0	96.6	87.9	1.00	4, 72
	*	20	-423	9.35	.368	365.5	53.0	165.5	24.0	158.7	144.4	1.00	4, 76
		20	-423	25.65	1.010	442.1	64.1	221.4	32.1	41.8	38.0	1.00	8, 104
		20	-423	25.53	1.005	442.1	64.1	221.4	32.1	52.9	48.1	1.00	8, 105
	*	20	-423	3.15	.124	456.6	66.2	209.0	30.3	104.7	95.3	1.00	8, 107
	*	20	-423	3.15	.124	456.6	66.2	209.0	30.3	73.2	66.6	1.00	8, 107
	*	77	-321	2.82	.111	296.6	43.0	151.7	22.0	432.9	393.9	1.00	4, 70
	*	77	-321	4.42	.174	296.6	43.0	151.7	22.0	256.3	233.2	1.00	4, 72
	*	77	-321	6.05	.238	296.6	43.0	151.7	22.0	186.7	169.9	.93	4, 74
	*	77	-321	8.97	.353	296.6	43.0	151.7	22.0	104.4	95.0	.76	4, 76
	*	77	-321	12.55	.494	296.6	43.0	151.7	22.0	105.1	95.6	1.00	4, 78
	*	77	-321	9.27	.365	296.6	43.0	151.7	22.0	75.7	68.9	.81	4, 78
		77	-321	25.91	1.020	382.1	55.4	184.8	26.8	77.3	70.3	1.00	8, 104
	*	77	-321	25.43	1.001	382.1	55.4	184.8	26.8	85.4	77.7	1.00	8, 104
	*	77	-321	3.10	.122	382.1	55.4	218.6	31.7	143.6	130.7	1.00	8, 106
	*	77	-321	3.12	.123	382.1	55.4	218.6	31.7	92.3	84.0	1.00	8, 106
2219-WELD						(SURFACE FLAW)							
	*	294	70	2.82	.111	241.4	35.0	124.1	18.0	285.3	259.6	1.00	4, 70
	*	294	70	4.37	.172	241.4	35.0	124.1	18.0	241.3	219.6	1.00	4, 72
	*	294	70	6.07	.239	241.4	35.0	124.1	18.0	276.0	251.1	1.00	4, 74
	*	294	70	8.97	.353	241.4	35.0	124.1	18.0	210.1	191.2	.95	4, 76
	*	294	70	12.55	.494	241.4	35.0	124.1	18.0	114.7	104.4	1.00	4, 78
	*	294	70	9.22	.363	241.4	35.0	124.1	18.0	68.0	61.9	.81	4, 79
	*	294	70	9.40	.370	241.4	35.0	124.1	18.0	346.7	315.5	.99	4, 83
	*	294	70	25.88	1.019	295.9	42.9	151.0	21.9	109.5	99.6	1.00	8, 103
	*	294	70	25.80	1.055	295.9	42.9	151.0	21.9	101.5	92.4	1.00	8, 103
	*	294	70	3.10	.122	266.2	38.6	184.1	26.7	242.7	220.8	1.00	8, 105
	*	294	70	3.12	.123	266.2	38.6	184.1	26.7	126.3	114.9	1.00	8, 105
	*	394	250	2.87	.113	206.9	30.0	110.3	16.0	20.2	18.4	0.00	4, 76
	*	394	250	4.45	.175	206.9	30.0	110.3	16.0	603.7	549.3	1.00	4, 72
	*	394	251	5.99	.236	206.9	30.0	110.3	16.0	369.6	336.3	.96	4, 74
	**	394	250	8.97	.353	165.5	24.0	110.3	16.0	--	--	--	4, 76
	**	449	350	5.92	.233	165.5	24.0	96.6	14.0	--	--	--	4, 74

Table 9. TENSILE PROPERTIES, FRACTURE CONSTANTS, AND TEST CONDITIONS FOR SURFACE- AND THROUGH-FLAW DATA. SI UNITS (U.S. CUSTOMARY UNITS)

MATERIAL & FLAW ORIENTATION	TEST TEMPERATURE °K	°F	NOMINAL THICKNESS MM	IN	ULTIMATE STRESS MN/m²	KSI	YIELD STRESS MN/m²	KSI	K_f MN/m$^{3/2}$	KSI√IN	M	REF., PAGE
2219-WELD					(THROUGH FLAW)							
*	20	-423	9.37	.369	365.5	53.0	165.5	24.0	57.1	52.0	.50	4, 77
*	77	-320	2.82	.111	296.6	43.0	151.7	22.0	1211.2	1102.1	1.00	4, 71
*	77	-320	4.39	.173	296.6	43.0	151.7	22.0	345.0	313.9	1.00	4, 73
*	77	-320	5.92	.233	296.6	43.0	151.7	22.0	97.2	88.4	.75	4, 75
*	77	-320	9.02	.355	296.6	43.0	151.7	22.0	246.5	224.3	1.00	4, 77
*	294	70	2.82	.111	241.4	35.0	124.1	18.0	286.7	260.9	1.00	4, 71
*	294	70	4.32	.170	241.4	35.0	124.1	18.0	291.2	265.0	1.00	4, 73
*	294	70	5.92	.233	241.4	35.0	124.1	18.0	330.8	301.0	1.00	4, 75
*	294	70	9.04	.356	241.4	35.0	124.1	18.0	145.6	132.5	.87	4, 77
**	394	250	2.84	.112	206.9	30.0	110.3	16.0	--	--	--	4, 71
*	394	250	4.37	.172	206.9	30.0	110.3	16.0	2230.2	2029.3	1.00	4, 73
**	394	250	5.89	.232	206.9	30.0	110.3	16.0	--	--	--	4, 75
*	394	250	8.94	.352	206.9	30.0	110.3	16.0	134.0	167.4	.86	4, 77
**	449	350	4.37	.172	165.5	24.0	96.6	14.0	--	--	--	4, 73
**	449	350	5.94	.234	165.5	24.0	96.6	14.0	--	--	--	4, 75

* Net stress exceeds yield stress

** Net stress exceeds ultimate stress

Table 10, 2219-T87 Aluminum Alloy Fracture Analysis Material Property Summary

Material Property \ Crack Propagation Direction / Thickness (cm) / Temperature	LT 0.127 (20K)	LT 0.127 R.T.	TL 0.127 (20K)	TL 0.127 R.T.	WELD 0.318 (20K)	WELD 0.318 R.T.
Ultimate Stress (MPa)	648	434	648	434	365	241
Yield Stress (MPa)	455	352	455	352	186	145
Cyclic Threshold Intensity (MPa $\sqrt{m}$)	6.6	3.8	6.6	3.8	**	**
C - Paris Coefficient (cm/cyc)/(MPa $\sqrt{m}$)^n	1.095E-21	1.489E-8	0.9675E-13	9.723E-9	2.089E-13	3.205E-10
n - Paris Exponent	13.0	2.8	12.4	2.8	8.5	5.2
Newman Parameters						
K_f (through crack) (MPa $\sqrt{m}$)	241	64.8	201	65.9	**	**
m (through crack) (MPa $\sqrt{m}$)	1.1	0	1.1	0	0	0
K_f (surface crack) (MPa $\sqrt{m}$)	192	50.6	160	44.0	**	**
m (surface crack) (MPa $\sqrt{m}$)	1.1	0	1.1	0	0	0

Table 10a. Selected References for Properties of 2219 Aluminum Alloy
(Numbers refer to reports listed under References)

	Thickness[1]	Temperature	Weldments
Strength	4[1]	4[1], 9	9[2], r[2]
Fatigue[2]			
Fracture Toughness	8	8, 9	5, 4[1]
Crack Growth	4[1]	4[1]	4[1]

Notes: (1) Data is available for thicknesses greater than 0.3175 cm. For thinner materials, very little data was available.

(2) Very little conventional fatigue data was avail ble for thin gauge 2219 at liquid hydrogen temperature. Some fatigue (and other) properties can be found in "Materials Data Handbook: Aluminum Alloy 2219," 2nd edition, R.F. Muraca and J. S. Whittick, NASA CR-123777, March 1972.

Table 11. Prediction Verification-Parent Metal at 20°K

(Stress Range 21-45 KSI)

	Specimen	Thickness (in)	Thickness (cm)	Width (in)	Width (cm)	Frequency (Hz)	Proof Tests	Cycles to Leak	Cycles to Break	Initial Crack Length (in)	Initial Crack Length (cm)
(Room temperature)	L8	.0518	.1306	4.012	10.190	1.0	0		*29496	0.2078	.5278
	L6	.0523	.1328	4.009	10.183	1.0	0	980	2043	0.2338	.5939
	L1	.0514	.1306	4.010	10.185	1.0	0	3246	7010		
	L2	.0516	.1311	4.010	10.185	1.0	1	3500	7160	0.2173	.5519
	L3	.0517	.1313	4.010	10.185	1.0	#1/1000	2930	8232	0.2177	.5530
	L5	.0516	.1311	4.000	10.160	1.0	0	120	2210		
	L9	.0515	.1308	4.010	10.185	1.0	1	3030	6360		
	L11	.0510	.1295	4.010	10.185	1.0	1/1000	3300	8946	0.2311	.5870
	L12	.0530	.1346	4.005	10.173	0.1	0	3145	8902	0.2126	.5400
	L14	.0517	.1313	4.000	10.160	0.1	1	3228	9816	0.2157	.5479
	L15	.0530	.1346	4.005	10.173	0.1	1/1000	2625	6966	0.2236	.5679
	L17	.0517	.1313	4.005	10.173	0.1	0	2400	6894	0.2268	.5761
	L18	.0511	.1298	4.002	10.165	0.1	1	3675	11200		
	L20	.0511	.1298	4.010	10.185	0.1	1/1000	3172	7690		

* Stress Ratio R = +0.1

\# One proof stress each 1000 cycles

Table 12. Prediction Verification-Weldments at 20°K

Stress Range 57.9 to 124.1 MPa (8.4 to 18.0 KSI)

Specimen	Frequency (Hz)	No. of Proofs	Cycles	
1-4V	1.0	1	135,000	No crack through
1-5V	1.0	1/1000 cycles	100,000	No crack through
2-4V	1.0	1	107,000	No crack through
3-2V	1.0	1/100	70,386	Pull rod failure, specimen deformed
3-4V	0.1	0	100,000	No crack through
4-1V	0.1	1	108,000	No crack through
5-1V	0.1	0	100,000	No crack through
5-5V	0.1	1	19,400	Failed in grip
6-1V	0.1	1/100	100,000	No crack through

Notes: Specimens 1-1V, 2-1V, 4-2V failed in grip during precracking

Table 13. Tensile Strength of 2219-T87 Aluminum Alloy

I	Condition	Test Temp. (°F)	Test Temp. (°K)	FTY (KSI)	FTY (MPa)	FTU (KSI)	FTU (MPa)	E 10^3(KSI)	E (MPa)	% (2" G. L.)	Remarks	Nominal thickness in.	Nominal thickness cm
*L1	Base Metal												
*L1	Metal	RT		56.3	388	66.9	461	10.6	63.1	8.5			
*L4		RT		56.7	391	67.2	463	10.1	69.6	8.5			
*L5		RT		55.6	383	66.2	456	10.5	72.4	9.0			
*T1		RT		56.1	387	67.5	465	11.0	75.8	8.0			
*T2		RT		55.6	383	66.6	459	10.0	68.9	8.5			
*T3		RT		55.4	382	66.2	456	10.5	72.4	6.5			
	Base												
*L6	Metal	-423	20	74.3	512	99.2	684	11.8	81.4				
*L7		-423	20	72.9	503	97.3	671	10.7	73.8	9.0			
*L9		-423	20	75.6	521	99.8	688			12.0			
*T5		-423	20	73.2	505	101	696	12.0	82.7	13.0			
*T6		-423	20	73.5	507	99.6	687	11.9	82.0	9.5			
*T7		-423	20	70.7	487	98.5	679			11.0			
1-1-T	Weldments	RT		19.6	135	38.5	265			4.0		.125	.318
2-1-T		RT		18.5	128	37.8	260			4.0		.125	.318
4-1-T		RT		20.6	142	37.9	261			3.5		.125	.318
3-1-T		-423	20	36.8	253	70.3	485			3.5		.125	.318
5-1-T		-423	20	32.6	225	68.6	473			4.5		.125	.318
6-1-T		-423	20	39.0	269	60.5	417			3.0		.125	.318
*L-3		-423	20	45.9	316	72.0	496			2.5		.050	.127
*L-8		-423	20	41.0	283	64.6	445			1.5		.050	.127

* Chem Milled

L = Longitudinal

T = Transverse

Table 14.

Plane Stress Crack Intensity Factor For
Chem-Milled 2219-T87 at Room Temperature. (Conventional Units)

Form	I.D.	B (in)	W (in)	2a (in)	P (K)	K_c (ksi $\sqrt{in}$)	
Base Metal	L3-1	.0536	2.938	0.81	5.68	42.7	
	L11-4	.0496	2.982	0.662	5.30	38.3	
	L10	.0516	3.984	1.055	7.70	50.4	
	L13	.0533	4.009	1.033	8.05	50.0	
	L16	.0530	4.010	1.035	7.86	49.0	
	T12-4	.0518	2.914	0.681	5.55	39.4	
	T13-3	.0507	2.905	0.682	5.10	37.1	
	T-1	.0530	4.018	1.129	6.80	44.7	
	T-2	.0535	4.016	1.129	7.15	46.6	
	T-3	.0530	4.015	1.111	7.22	47.1	
Weld (All Long)	W-4	.0530	4.010	0.980	4.95	30.0	*
	2-2D	.1303	4.005	1.097	11.00	29.1	
	3-3D	.1281	3.980	1.064	11.50	30.5	
	4-4D	.1257	3.998	1.107	11.20	30.9	
	3-5D	.1305	3.994	1.108	11.50	30.6	
	6-3D	.1247	4.022	1.083	11.50	30.6	

*Damaged during precracking

Table 15

Plane Strain Stress Intensity Factor for Chem Milled
2219-T87 at Room Temperature
(SI Units)

Form	I.D.	B (cm)	W (cm)	2a (cm)	P (MN)	K_c (MPa $\sqrt{m}$)
Base Metal	L3-1	.136	7.463	2.057	.0252	46.9
	L11-4	.126	7.574	1.681	.0235	42.1
	L10	.131	10.119	2.680	.0341	55.4
	L13	.135	10.183	2.624	.0357	54.9
	L16	.135	10.185	2.629	.0349	53.8
	T12-4	.132	7.402	1.730	.0246	43.3
	T13-3	.129	7.379	1.732	.0226	40.8
	T-1	.135	10.206	2.868	.0302	49.1
	T-2	.136	10.201	2.868	.0317	51.2
	T-3	.135	10.198	2.822	.0320	51.8
Weld	W-4	.135	10.185	2.489	.0220	33.0
	2-2D	.331	10.173	2.786	.0488	32.0
	3-3D	.325	10.109	2.703	.0510	33.5
	4-4D	.319	10.155	2.812	.0497	34.0
	3-5D	.332	10.145	2.814	.0510	33.6
	6-3D	.317	10.216	2.751	.0510	33.6

Table 16.

Plane Stress Crack Intensity Factor for 2219 T87
Aluminum Alloy at -423°F (conventional units)

Form	I.D.	B (in)	W (in)	2a (in)	P (K)	G (ksi)	Kc (ksi $\sqrt{in}$)	
Base Metal	L23	.0515	4.005	1.087	9.500	46.01	63.0	
	L24	.0517	4.005	1.086	9.375	45.27	62.0	
	L25	.0517	4.006	1.085	9.500	45.87	62.7	
	L26	.0514	4.007	1.082	9.600	46.61	63.7	
	L27	.0517	4.008	1.083	9.500	45.85	62.7	
	T4	.0527	4.010	1.124	8.925	42.23	64.6	
	T5	.0527	4.021	1.118	9.500	44.83	63.8	
	T6	.0520	4.020	1.139	9.000	43.05	60.6	
	T7	.0510	4.016	1.173	8.700	42.48	60.6	
	T8	.0495	4.015	1.119	8.500	42.77	59.6	
Weld	W1	.0522	4.026	1.065	6.65	31.64	42.8	(1)
	W2	.0525	3.997	1.052	7.25	34.55	42.5	(1)
	2-5D	.1315	3.979	1.052	14.55	27.80	37.4	(2)
	5-3D	.1290	4.000	1.132	15.10	29.26	41.1	
	6-2D	.1295	3.993	1.090	15.40	29.78	40.9	

(1) Chem Milled
(2) Grip Failure

Table 17

Plane Stress Crack Intensity Factor for 2219-T87
Aluminum Alloy at 20°K
(SI Units)

Form	I.D.	B (cm)	W (cm)	2a (cm)	G (MPa)	K_c (MPa $\sqrt{m}$)	
BM	L23	.1308	10.173	2.761	317.2	69.2	
	L24	.1313	10.173	2.758	312.1	68.1	
	L25	.1313	10.175	2.756	316.3	68.9	
	L26	.1306	10.178	2.748	321.4	70.0	
	L27	.1313	10.180	2.751	316.1	68.9	
	T4	.1339	10.185	2.855	291.2	71.1	
	T5	.1339	10.213	2.840	309.1	70.1	
	T6	.1321	10.211	2.893	296.8	66.6	
	T7	.1295	10.201	2.954	292.9	66.6	
	T8	.1257	10.198	2.842	294.9	65.5	
Weld	W1	.1326	10.226	2.705	218.2	47.1	Chem milled
	W2	.1334	10.152	2.672	238.2	46.8	Chem milled
	2-5D	.3340	10.107	2.672	191.7	41.1	Grip failure
	5-3D	.3277	10.160	2.875	201.7	45.2	
	6-2D	.3289	10.142	2.69	205.3	45.0	

APPENDIX A

GROWTH OF SURFACE FLAWS AND THRU CRACKS IN WIDE PLATES (an H-P 9830 Program)

This program does a cycle-by-cycle integration of crack growth in wide plates in the thickness direction, a, and the length direction, C. The growth rate equation used in the program is shown below and is basically that developed by Collipriest and Ehret (Ref. 1). The two parameter fracture criterion, Eq. 2, developed by Newman (Ref. 2), is used both in the growth rate equation to define the upper limit of stable crack growth, and to check the applied stress intensity factor for criticality. Eq. 3, also due to Newman (Ref. 3), defines the elastic magnification of the stress intensity factor for surface cracks.

$$da/dN = C_1 \text{ EXP} \left[C_2 \text{ TANH}^{-1} \left(\frac{\ln (\Delta K^2 / ((1 - R)K_c \Delta K_0))}{\ln ((1 - R)K_c/\Delta K_0))} \right) \right] \quad (1)$$

where K_c = Critical stress intensity factor for cyclic growth

ΔK_0 = Threshold stress intensity range

C_1 = Growth rate intercept; da/dN at inflection point

C_2 = Dimensionless coefficient relating to midrange slope

and

da/dN = Fatigue crack extension per load cycle

ΔK = Applied stress intensity range $(K_{max} - K_{min})$

R = Load ratio (minimum load/maximum load)

also

$$C_2 = \ln (K_c/\Delta K_0)^{n/2}$$

$$C_1 = C (K_c \Delta K_0)^{n/2}$$

where C and N are the Paris Equation coefficient and exponent.

$$K_{Ie} = K_f\ (1 - m(S_n/\sigma_u)) \qquad (2)$$

where K_{Ie} = Elastic stress intensity factor at failure assumed equal to K_c defined above

K_f = Newman fracture toughness

m = Newman fracture toughness parameter

S = Net section stress

σ_u = Ultimate tensile strength

$$M_e = M_1 + \left(\sqrt{Q\frac{c}{a}} - M_1\right)\left(\frac{a}{t}\right)^p \qquad (3)$$

where

$$p = 2 + 8\left(\frac{a}{c}\right)^3$$

$$Q = 1 + 1.47\left(\frac{a}{c}\right)^{1.64} \quad \text{for } \frac{a}{c} \le 1.0$$

$$Q = 1 + 1.47\left(\frac{c}{a}\right)^{1.64} \quad \text{for } \frac{a}{c} > 1.0$$

$$M_1 = \sqrt{\frac{c}{a}}\left(1 + 0.03\frac{c}{a}\right) \quad \text{for } \frac{a}{c} > 1.0$$

$$M_1 = 1.13 - 0.1\left(\frac{a}{c}\right) \text{ for } 0.02 \le \frac{a}{c} \le 1.0$$

The predictive accuracy of the program has not been verified; however, it is the only known program to contain a rational treatment of all of the following effects:

a. The lower threshold of growth
b. The upper limit of stable growth
c. Thickness effect on growth rate
d. Thickness effect on K critical
e. Elastic magnification of K for surface flaws
f. Proof test

Since the H-P 9830 is interactive (i.e., questions are displayed to which the user responds), a user guide is not needed. However, the following notes and sample output may be helpful.

NOTES:

1. A maximum of 5 segments may be input. This is limited by computer memory of 3808 words.
2. Two sets of material properties may be specified. (Displayed as Temp 1 and Temp 2)
3. The transition from PTC to TC is abrupt, i.e., when a =t the program shifts to a TC of length .75 × 2C. This will not be significant for thin, tough materials. For thicker plates some transition growth correction is needed.
4. As a user option a ground-air-ground, G-A-G cycle may be automatically generated if:
   a. Three or more segments are input.
   b. At least one of the segments used is a ground condition and at least one other is a flight condition. (Segment 1 is not used in GAG to avoid applying proof test twice at start.)
5. Cycles occurring less than once per flight are distributed as follows:
   a. If in Segments 1, 3, or 5 are applied on the first flight and at the specified frequency.
   b. If in Segments 2 or 4 are not applied on first flight but at specified frequency thereafter.
6. Segment 1 should be used for proof test(s). See Notes 4 and 5 above.
7. Run time is very slow if a full 5 segment spectrum is run. As a rough estimate assume each cycle requires 2 to 3 seconds.

References:

1. Collipriest, J. E., and Ehret, R. M., "Computer Modeling of Part Through Crack Growth", Space Division, Rockwell International Corporation, SD-72-CE-0015B (Oct. 1973).
2. Newman, J. M., "Plane-Stress Fracture of Compact and Notch-Bend Specimens", NASA TM X-71926, Feb. 1974.
3. Newman, J. M., "Fracture Analysis of Surface and Through-Cracked Sheets and Plates", Engineering Fracture Mechanics, 1973, Vol. 5, pp. 667-689, Pergamon Press.

MPLE OUTPUT

**** GROWTH OF SURFACE FLAWS AND THRU CRACKS IN WIDE PLATES ****

OMETRY

te Thickness (cm) =	0.10
ial Flaw Depth (cm) =	0.076
w Half Length (cm) =	0.635

TERIAL PROPERTIES	TEMP 1	TEMP 2
Strength = (MPa)	434	648
Stress Intensity (MPa $\sqrt{m}$) =	3.85	6.04
ris Coef. C. (cm/cycle)/(MPa $\sqrt{m}$)^n =	4.07545E-09	1.43191E-11
ris Exponent, N =	3.3	4.82
wman Param, KF, for TC (MPa $\sqrt{m}$) =	280	227
wman Param, M, for TC =	1	1
wman Param, KF, for PTC MPa $\sqrt{m}$	199	180
wman Param, M, for PTC =	1	1

RESS SPECTRUM

. Segments in Flight =	5
. Flights in Req'd. Life =	100
tter Factor =	2
. Flights in Print Interval =	1
to Generate G-A-G Cycle =	1

GMENT NO.	MAXIMUM STRESS	MINIMUM STRESS	CYCLES PER FLIGHT	TEMP NO.
1	344.7	0.00	0.010	1
2	137.9	0.00	0.100	1
3	82.73	55.15	1.000	2
4	275.8	103.4	0.785	2
5	310.3	68.95	0.205	2

IGHT	A	C	DELTA KA	DELTA KC	MAX KA	MAX KC	CRIT K
0	0.0762	0.6350					
1	0.0810	0.6350	35.39	6.40	35.39	6.40	41.04
2	0.0810	0.6350	26.56	4.34	30.22	5.43	103.52
3	0.0813	0.6350	24.24	4.35	30.31	5.44	103.52
4	0.0815	0.6350	24.32	4.36	30.39	5.46	103.52
5	0.0828	0.6350	27.83	5.09	34.53	6.19	93.94

AMPLE OUTPUT (Continued)

LIGHT	A	C	DELTA KA	DELTA KC	MAX KA	MAX KC	CRIT K
14	0.0881	0.6350	3.32	0.59	9.97	1.77	157.20
15	0.0914	0.6350	31.27	5.54	38.03	6.74	93.94
16	0.0925	0.6350	27.75	4.89	34.68	6.12	103.52
17	0.0932	0.6350	28.03	4.93	35.03	6.18	103.52
18	0.0942	0.6350	28.34	4.99	35.42	6.23	103.52
19	0.0942	0.6350	3.57	0.63	10.72	1.88	157.2
REAKTHRU THICKNESS - LEAK							
20	0.1062	0.6350	41.73	7.28	41.72	7.28	71.96
20	0.1016	0.4763	41.73	7.28	41.73	7.28	71.96
21	0.1016	0.4763	0.00	26.99	0.00	33.73	130.66
22	0.1016	0.4763	0.00	27.00	0.00	33.74	130.66
137	0.1016	0.7816	0.00	39.53	0.00	48.07	118.57
138	0.1016	0.7871	0.00	34.60	0.00	43.25	121.87
139	0.1016	0.7927	0.00	34.72	0.00	43.40	130.66
140	0.1016	0.7927	0.00	21.77	0.00	21.77	179.07
141	0.1016	0.7988	0.00	34.86	0.00	43.57	130.66
142	0.1016	0.8446	0.00	40.91	0.00	99.77	118.57
143	0.1016	0.8532	0.00	35.99	0.00	44.98	130.66
144	0.1016	0.8623	0.00	36.17	0.00	45.22	130.66
145	0.1016	0.8623	0.00	4.54	0.00	13.61	198.42
146	0.1016	0.8720	0.00	36.36	0.00	45.46	130.66
147	0.1016	0.9528	0.00	43.03	0.00	52.34	118.57
148	0.1016	0.9700	0.00	38.25	0.00	47.82	130.66
149	0.1016	0.9700	0.00	4.81	0.00	14.44	198.42
150	0.1016	1.009	0.00	48.26	0.00	48.26	121.87
151	0.1016	1.033	0.00	39.39	0.00	49.24	130.66
152	0.1016	1.320	0.00	48.09	0.00	58.48	118.57
153	0.1016	1.458	0.00	45.49	0.00	56.87	130.66
154	0.1016	1.458	0.00	5.90	0.00	17.70	198.42
155	0.1016	1.749	0.00	48.26	0.00	60.33	130.66
156	0.1016	3.421	0.00	55.04	0.00	68.80	130.66
NSTABLE GROWTH IN C DIRECTION							
157	0.1016	103.8151	0.00	435.8	0.00	560.33	118.57

REFERENCES

1. Collipriest, J. E. and Ehret, R. M., "Computer Modeling of Part Through Crack Growth," Space Division, Rockwell International Corporation, SD-72-CE-0015B, October 1974.

2. Newman, J. C., "Plane-Stress Fracture of Compact and Notch-Bend Specimens," NASA TM X-71926, February 1974.

3. Newman, J. C., "Fracture Analysis of Surface and Through-Cracked Sheets and Plates," Engineering Fracture Mechanics, 1973, Vol. 5, pp 667-689, Pergamon Press.

4. Fiftal, C. F., "Fracture Mechanics Data on 2219-T87 Aluminum for the Space Shuttle External Tank," Martin Marietta Corporation, Test Report No. 826-2027.

5. General Dynamics Convair, "Investigations of Light Weight Designs and Materials for LO_2 and LH_2 Propellant Tanks for Space Vehicles, Interim Report, Phase I," Convair Report No. PD75-0117, December 1975.

6. Orange, T. W., Sullivan, and Calfo, "Fracture of Thin Sections Containing Through and Part-Through Cracks," NASA TM X-52794, June 1970.

7. Engstrom, W. L., "Effect of Thermal Profile in Cyclic Flaw Growth in Aluminum," NASA CR-134679, January 1975.

8. Masters, J. N., "Investigation of Deep Flaws in Thin Walled Tanks," NASA CR-72606, December 1969.

9. Engstrom, W. L., "Determination of Design Allowable Properties - Fracture of 2219-T87 Aluminum Alloy," NASA CR-114388, March 1972.

10. Materials Properties Manual, Vol. 1, Design Data, Rockwell International/ Space Division, 2543 W, June 1975.

BIBLIOGRAPHY

Adams, N. J. I., "Fatigue Crack Closure at Positive Stresses," Engineering Fracture Mechanics, Vol. 4., Sept. 1972, p. 543-554.

Aerojet General Corp., Materials Properties Data Book, Vol. 4, NASA-CR-131813.

Aerojet General Corp., Materials Properties Data Book, Vol. 4, NASA-CR-131814.

Aerojet General Corp., Materials Properties Data Book, Addendum, NASA-CR-131816.

Anderson, W. F., "Fracture Mechanics of Tiny Cracks Near Fasteners," ASD-TR-74-24.

Babilon, C. F., Wygonik, R. H., Nordmark, G. E., and Lifka, B. W., "Mechanical Properties, Fracture Toughness, Fatigue, Environmental Fatigue Crack Growth Rates and Corrosion Characteristics of High Toughness Al Alloy Forgings, Sheet and Plate," AFML-TR-73-83.

Bjeletich, J. G., Morton, T. M., and Lewis, R. E., "Welding Fracture Toughness of an Aluminum-Copper Alloy," Welding Journal, Research Supplement, Vol. 53, April 1974, p. 153-5 to p. 160-5.

Buch, A., "Notch Sensitivity and Fatigue Strength of Aircraft Sheet Material Specimens," Israel Institute of Tach, Haifa, TAE-184.

Brainshaw, F. J. and Wheeler, C., "The Crack Resistance of Some Aluminum Alloys and the Prediction of Thin Section Failure," Royal Aircraft Establishment, Farnborough, England, RAE-TR-73191.

Campbell, J. E., "Fracture Toughness of High Strength Alloys at Low Temperature-A Review," A75-12012, 02-26, ASIM 1974, p. 3-20.

Crooker, T. W., "The Role of Fracture Toughness in Low-Cycle Fatigue Crack Propagation for High Strength Alloys," Engineering Fracture Mechanics, Vol. 5, Feb. 1973, p. 35-43.

Crooker, T. W., "Fatigue and Corrosion Fatigue Crack Propagation in Intermediate-Strenth Al Alloys," Journal of Engineering Materials and Technology, Vol. 95, July 1973, p. 150-156.

Czyryca, E. J. and Vissilaros, M. G., "Engineering Properties of Structural Al Alloys, A Handbook," Naval Ship Research & Development Center, Annapolis, Md., NSRDC-8-967, NSRDC-3571.

Davies, K. B. and Fedeersen, C. E., "Evaluation of Fatigue-Crack Growth Rates by Polynomial Curve Fitting," International Journal of Fracture, Vol. 9, March 1973, p. 116-118.

Engstrom, W. L., "Study of Deep Flaws in Weldments of Aluminum and Titanium," NASA-CR-128264.

Engstrom, W. L., "Study of Deep Flaws in Weldments of Aluminum and Titanium" NASA-CR-129418.

Erhardt, K., Wilson, A., Pelloux, R. M. N. and Grant, N. J., "Mechanics of Fatigue Crack Propagation in Aluminum Alloys," AFML-TR-71-109.

Fitzgerald, J. H. and Wei, R. P., "A Test Procedure for Determining the Influence of Stress Ratio on Fatigue Crack Growth," Journal of Testing and Evaluation, Vol. 2, March 1974, p. 67-70.

Garret, G. G. and Knott, J. F., "On the Influence of Fracture Mechanisms on Fatigue Crack Propagation in Aluminum Alloys," Metallurgical Transactions A, Physical Met. & Materials Science, Vol. 6A, Aug. 1975, p. 1663-1665.

Gest, R. J. and Troiano, A. R., "Stress Corrosion and Hydrogen Embrittlement in an Aluminum Alloy," Corrosion, Vol. 30, Aug. 1974, p. 274-279.

Goode, R. J. and Judy, R. W., Jr., "Application of Principles for Fractures-Safe Design for Aluminum and Titanium Alloys," Welding Journal, Research Supplement, Vol. 53, March 1974, p. 135-5 to p. 143-5.

Hahn, G. T. and Simon, R., "Metallurgical Control of Fatigue Crack Growth in High-Strength Al Alloys," AFML-TR-72-48.

Hahn, C. T. and Simon, R., "A Review of Fatigue Crack Growth in High Strength Al Alloys and the Relevant Metallurgical Factors," Engineering Fracture Mechanics, Vol. 5, Sept. 1973, p. 523-540.

Hall, L. R., "Investigation of Stress and Chemical Environments on the Prediction of Fracture in Aircraft Structural Materials," 73X80726-BR 113710, Boeing, Seattle, Washington.

Hall, L. R. and Bixler, W. D., "Subcritical Crack Growth of Selected Aerospace Pressure Vessel Materials," NASA-CR-120834.

Hall, L. R. and Finger, R. W., "Investigation of Flaw Geometry and Loading Effects on Plane Strain Fracture in Metallic Structures," NASA-CR72659.

Hall, L. R. Shaw, R. C. and Engstrom, W. L., "Fracture and Fatigue Crack Growth Behavior of Surface Flaws & Flaws Originating at Fastener Holes," Vol. 1, Results and Discussion., AFFDL-TR-74-47.

Hoeppner, D. W. and Goss, G. L., "A Fretting-Fatigue Damage Threshold Concept," Wear, Vol. 27, Jan. 1974, p. 61-70.

Hyatt, M. V., "Program to Improve the Fracture Toughness and Fatigue Resistance of Al Sheet and Plate for Airplane Application," AFML-TR-73-224.

Hyatt, M. V. and Speidel, M. O., "Stress-Corrosion Cracking of High-Strength Aluminum Alloys," 73X74744, BR564481, Boeing Co., Seattle, Wash.

Jones, D. L. Liebowitz, H. and Eftis, J., "Fracture Toughness Characterization of Several Al Alloys in Semi Brittle Fracture," Engineering Fracture Mechanics, Vol. 6., Dec. 1974, p. 639-652.

Johnson, F. A. and Radon, J. A., "Strain Rate-Crack Speed Relation in Steady State Fracture Processes," International Jo. of Fracture, Vol. 10,

Judy, R. W., Jr. and Griffis, C. A., "Fracture Extension Resistance of Al. Alloys in Thin Sections," NRL-7627.

Ke, J. S., "Crack Tip Deformation and Ductile Fracture Criteria," S8637272, Syracuse University.

Kramer, I. R., "The Influence of Environment on Crack Behavior," AFOSP-74-1908-TR.

Lawrence, F. V., "Effects of Porosity on the Fatigue Behavior of Al Alloy Weldments," N00024-73-C-5344.

Liu, A. F., "Crack Growth and Failure of Al Plate Under In-Plane Shear," AIAA Journal, Vol. 12, Feb. 1974, p. 180-185.

Masters, J. N. Bixler, W. D. and Fingers, R. W., "Fracture Characteristics of Structural Aerospace Alloys Containing Deep Surface Flaws," NASA-CR-134587.

National Aeronautical Lab-Bangalore (India), "Fatigue Crack Propagation-Aluminum & Titanium Alloys, Steel and Reinforced Plastics-An Annotated Bibliography"(1968-1972), NAL BIBL-SER-40.

Newman, J. C. Jr., "Fracture Analysis of Various Cracked Configurations in Sheet and Plate Materials," NASA-TMX-72-709.

Nordmark, G. E. and Kaufman, J. G., "Fatigue-Crack Propagation Characteristics of Al Alloys in Thick Sections," Engineering Fracture Mechanics, Vol. 4, June 1972, p. 193-204.

Ogura, T. Karashima, S. and Tsurukame, K., "Propagation of Fatigue Cracks in Aluminum at Low Temperatures," Japan Institute of Metals Transactions, Vol. 16, Jan. 1975, p. 43-48.

Pearson, S., "Initiation of Fatigue Cracks in Commercial Aluminum Alloys and Subsequent Propagation of Very Short Cracks," Engineering Fracture Mechanics, Vol. 7, June 1975, p. 235-247.

Pettit, D. E. and Hoeppner, D. W., "The Effect of Initial Flaw Configuration on Leak Critical Pressure Vessel Design," AIAA-Structures & Materials Conf. 16th, Denver, 27 May 1975, AIAA Paper 75-803.

Pook, L. P., "Fatigue Crack Growth Data for Various Materials Deduced from the Fatigue Lives of Pre-cracked Plates," National Symposium on Fracture Mechanics, 5th, Urbana, Ill., August 31-Sept. 2, 1971.

Reifsnider, K. and Kahl, M., "Effect of Local Yield Strength Gradients on Fatigue Crack Propagation," I. F. of M. S., Vol. 16, Feb. 1974, p. 105-119.

Rice, R. C. and Jaskie, C. E." Consolidated Presentation of Fatigue Data for Design Applications," S. of A. E., Feb. 25-March 1, 1974, SAE Paper No. 740277.

Ruff, P. E. and Hyler, W. S., "The Collection, Generation, and Analysis of MIL-HDBK-5 Allowable Design Data," AFML-TR-74-67.

Shah, R. C., "Effects of Proof Loads and Combined Mode Loadings on Fracture and Flaw Growth Characteristics of Aerospace Alloys," NASA-CR-1346111.

Schmidt, R. A., "Extremely Low Fatigue Crack Propagation," 73N27779 LK410779.

Shih, T. T. and Wei, R. P., "A Study of Crack Closure in Fatigue," Engineering Fracture Mechanics, Vol. 6, Mar. 1974, p. 19-32.

Shiratori, E. and Obataya, Y., "Cyclic Creep-Type Fracture and Fatigue-Type Fracture in the Constant Load Low Cycle Fatigue Tests," I. J. of M. S., Vol. 16, July 1974, p. 433-447.

Shults, J. M., "Materials Selection and Evaluation for Advanced Metallic Aircraft Structures," AIAA Paper No. 74-373.

Sprowls, D. O., Shumaker, M. B., Walsh, J. D. and Coursen, J. W., "Evaluation of Stress Corrosion Cracking Susceptibility Using Fracture Mechanics Techniques, Part I," NASA-CR-124469.

Stadnick, S. J., "Fatigue Crack Initiation as a Function of Temperature and Strain Rate," THM-382.

Staley, J. T., "Stress-Corrosion Cracking in Aluminum Alloys," Metals Engineering Quarterly, Vol. 13, Nov. 1973, p. 52-57.

Stephens, R. I., McBurney, G. W. and Oliphant, L. J., "Fatigue Crack Growth with Negative R Ratio Following Tensile Overloads," International Jo. of Fatigue, Vol. 10, Dec. 1974, p. 587-589.

Sullivan, A. M. and Stoop, J., "Some Fracture Mechanics Relationships for Thin Sheet Materials," Naval Research Laboratory, Washington, D. C., NRL-7650.

Sullivan, A. M., Stoop, J. and Freed, C. N., "Influence of Sheet Thickness Upon the Fracture Resistance of Structural Al Alloys," Progress in Flaw Growth and Fracture Toughness Testing-Proceedings of the 6th National Symposium on Fracture Mechanics, Philadelphia, Pa., Aug. 28-30, 1972.

Volkov, V. A., Markovets, M. P. Drozdovskii, B. A. and Polishchuk, T. V., "Fracture Toughness Testing of High Strength Aluminum Alloy," Proceedings 5th An. Congress on Material Testing, Budapest, Hungary, Oct /Nov. 1964, Vol. 1, Akademiai Krado, 1974.

Wang, D. Y., "Plane-Stress Fracture Toughness and Fatigue Crack Propagation of Al. Alloy Wide Panels," Progress in Flaw Growth and Fracture Toughness Testing-Proceedings of the 6th National Symposium on Fracture Mechanics, Philadelphia, Pa., August 28-30, 1972.

Williams, D. N., "A Review of Subcritical Crack Growth Under Sustained Load," AIAA Paper No. 75-804, Structures and Materials Conference, Denver, 27 May 1975.